

Moderator Displacers for Reducing Coolant Void Reactivity in CANDU Reactors: A
Neutronics Scoping Study

by

Robert Farkas

A Thesis Submitted in Partial Fulfillment
of the Requirements for the Degree of

Master of Applied Science

In

Nuclear Engineering

University of Ontario Institute of Technology

August 2014

© Robert Farkas, 2014

Placeholder for the Certificate of Approval

Abstract

When the coolant is voided in a CANDU lattice, the net reactivity change is positive, due primarily to the fact that the coolant and moderator are separated and the coolant volume is much smaller than the moderator volume. The modest loss in moderation occurring when coolant is lost does not offset the positive reactivity contributions of increased fast fission rate and reduced epithermal absorption. A way to achieve a negative net reactivity effect on coolant voiding is to increase the importance of moderation in the coolant by decreasing the moderator-to-coolant volume ratio. This work proposes to reduce the moderator-to-coolant volume ratio in existing CANDU reactors by packing the moderator with displacers in the shape of close-packed hollow spheres. Results show that it is possible to reduce the coolant void reactivity through the use of spherical moderator displacers, albeit at a cost in discharge burnup.

Acknowledgement

I wish to thank Dr. Rouben and Dr. Harvel for their generosity in the form of time and expertise as members of my supervisory committee – their feedback on my work was exceedingly valuable. Equally, I wish thank Dr. Whitlock for taking the time to perform the external review of my thesis and allowing it to benefit from his considerable knowledge of the subject matter. Similarly, I owe thanks to Dr. Buijs who instigated my return to graduate school. This work also relied on non-academic support and for that I thank my wife.

Finally, I am indebted to my graduate supervisor Dr. Nichita. I have been fortunate for his ingenuity and steady guidance during the oversight of my project. Over the years I have been most surprised with his unwavering patience which by some marvel I was unable to deplete.

Contents

Chapter I Introduction	1
Chapter II Features of CANDU Coolant Void Reactivity	6
Chapter III Review of Design Elements Intended to Manipulate Reactor Coolant Density Reactivity Coefficient	14
Chapter IV Methodology and Modelling Considerations	34
Chapter V Close-Packed Moderator Displacers	49
Chapter VI Conclusions	78
Chapter VII Future Work	80
References	83
Appendix A Example DRAGON Input File	86

Figures

Figure 1 Components of a CANDU lattice.	1
Figure 2 Typical CANDU6 lattice cell containing a 37-element fuel bundle in a) the cooled state and b) the voided state.	2
Figure 3 Reactivity dependence on the amount (mass) of moderator within the lattice cell.	7
Figure 4 Comparison of the reactivity dependence on the amount (mass) of moderator within the fresh lattice cell between the cooled and voided cell.	8
Figure 5 Comparison of the reactivity dependence on the amount (mass) of moderator within a mid-burnup lattice cell between the cooled and voided cell.	9
Figure 6 Coolant void reactivity as a function of burnup, presented from fresh to approximately mid-burnup fuel.	10
Figure 7 Change in fuel flux on voiding (solid) and the plutonium-239 production cross-section (dashed) with a resonance at approximately 0.3 eV.	10
Figure 8 Difference (voided less cooled) in thermal (below 0.625 eV) flux within a fresh CANDU lattice (arbitrary units).	12
Figure 9 Difference (voided less cooled) in fast (above 0.625 eV) flux within a fresh CANDU lattice (arbitrary units).	13
Figure 10 Core layout of the prototype SGHWR at Winfrith.	15
Figure 11 Experimental apparatus of a) a small annular void can and b) a larger annular void can	17
Figure 12 Comparison of 19-element fuel bundle a) and 37-element fuel bundle b).	17
Figure 13 Bundle Geometries modified by eliminating the central elements to reduce coolant void reactivity. a) Modified 37-element bundle (with 30 elements) and b) modified 61-element bundle (with 42 elements).	19
Figure 14 Comparison of bundle geometries a) 43-element bundle with large centre pin b) standard 37-element bundle.	22
Figure 15 Standard 37-element bundle with elements a) having a graphite core and b) being surrounded by a graphite annulus	25
Figure 16 Annular fuel bundle.	27
Figure 17 Scale comparison of a) the traditional 37-element CANDU lattice and b) the 78-element PT-SCWR lattice.	32
Figure 18 Three-dimensional lattice cell (a) without displacers and (b) with displacers.	34
Figure 19 DRAGON models of (a) a typical CANDU lattice and (b) a CANDU lattice cell with displacers.	39
Figure 20 Graphical summary of the calculation methodology.	40
Figure 21 Comparison of mechanisms for reducing CVR (2.0 wt% fuel enrichment; 0.00 cm displacer thickness).	42
Figure 22 Burnup averaged reactivity curve for the nominal CANDU lattice.	44
Figure 23 Flowchart depicting the scoping study methodology.	49
Figure 24 Change in fuel flux on voiding for both the fresh nominal (black) and fresh lattice with displacers (grey).	50
Figure 25 Burnup averaged coolant void reactivity for zirconium displacers.	51
Figure 26 Discharge burnup for zirconium displacers.	52
Figure 27 Burnup averaged coolant void reactivity for graphite displacers.	55
Figure 28 Discharge burnup for graphite displacers.	55

Figure 29 Burnup averaged coolant void reactivity for beryllium displacers.	57
Figure 30 Discharge burnup for beryllium displacers.....	58
Figure 31 Burnup averaged coolant void reactivity for lead displacers.....	59
Figure 32 Discharge burnup for lead displacers.	60
Figure 33 Energy dependence of the microscopic absorption cross-section for lead.	61
Figure 34 Energy dependence of the microscopic absorption cross-section for zirconium.....	62
Figure 35 Difference in absorption rate, voided less cooled, as a function of position in the 2.0 wt% enriched lattice with 0.05 cm zirconium displacers.....	63
Figure 36 Difference in absorption rate, voided less cooled, as a function of position in the 2.0 wt% enriched lattice with 0.05 cm lead displacers.	64
Figure 37 Burnup averaged coolant void reactivity for aluminum displacers.	65
Figure 38 Discharge burnup for aluminum displacers.	66
Figure 39 Checker-board pattern voiding of coolant in a 2×2 cell model – diagonal cells are voided.....	68
Figure 40 Coolant void reactivity in a displaced lattice cell with graded enrichment.	74
Figure 41 Discharge burnup in a displaced lattice cell with graded enrichment.	74
Figure 42 A layered displacer where each color represents a different material.	81
Figure 43 A distribution of displacers where each color represents a different material.....	81

Tables

Table 1 Coolant Void Reactivity Reductions for Bundles Illustrated in Figure 13	19
Table 2 Intra-bundle Grading of Enrichment and Burnable Neutron Poison for Zero Void Reactivity Lattice	20
Table 3 Influence of the Coolant Composition on the Thermal Flux within the Fuel on Voiding of the Coolant	21
Table 4 Parametric Study of Coolant Void Reactivity and Dysprosium Content in the Large Centre pin of a 43-element Bundle with Depleted Uranium in the Innermost Two Rings and Enriched Uranium in the Outermost Two Rings.....	23
Table 5 Parametric Study of Coolant Void Reactivity and Dysprosium Content in the Large Centre Pin of a 43-element Bundle with Uniformly Enriched Fuel.....	23
Table 6 Effect of Graphite Core within the Elements of a 37-element bundle	26
Table 7 Effect of Graphite Annulus around the Elements of a 37-element bundle	26
Table 8 Comparison of a 37-element Bundle with Depleted Uranium and Dysprosium Inner Rings and Graphite and Dysprosium Inner Element.....	29
Table 9 Comparison of a 43-element Bundle with Large Centre Pin with Depleted Uranium and Dysprosium Inner Rings and Graphite and Dysprosium Inner Element.....	30
Table 10 Macroscopic Cross-sections and Atomic Weights for 2200 m/s neutrons for Select Materials	45
Table 11 Buckling Pressure for Select Materials	47
Table 12 Summary of CBCVR and full-void CVR for Various Materials at a Thickness of 0.02 cm and Fuel Enrichment of 2.0 wt%	68
Table 13 Price Components of Nuclear Fuel (year 2011)	71
Table 14 Relative Fuel Cost for Different Displacer Materials (0.02 cm displacer wall-thickness)	72
Table 15 Comparison of the Cost in Terms of Discharge Burnup of Different Means of Reducing CVR in a CANDU Lattice with Close-packed Displacers.....	76

Chapter I Introduction

CANDU reactors currently in operation are large thermal reactors both cooled and moderated by heavy water. The CANDU core is composed of a square lattice of horizontal fuel channels immersed in a low-temperature low-pressure moderator. Each fuel channel consists of two concentric tubes. The inner tube, called the pressure tube, comprises part of the pressure boundary for the high-temperature high-pressure coolant and contains a string of fuel bundles. The outer tube, called the calandria tube, has an outer surface in contact with the moderator and an inner surface separated from the pressure tube by a gas filled annulus gap. The entire array of fuel channels is surrounded by a region of heavy water serving as a reflector and is enclosed in a horizontal cylindrical vessel, called the calandria. A two-dimensional lattice cell is defined as a cross-section through the channel, with enough moderator to complete a square concentric with the fuel channel, and with side equal to the distance between channels, called the lattice pitch. A two-dimensional lattice cell is depicted in **Figure 1**.

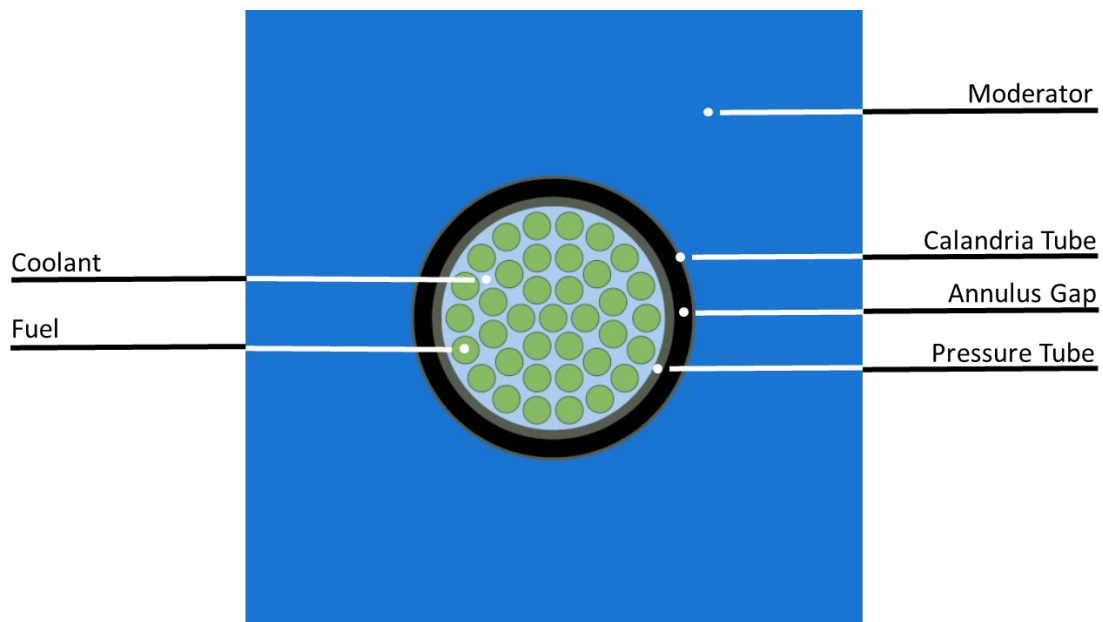


Figure 1 Components of a CANDU lattice.

Unlike the situation in Pressurized Water Reactors, in the CANDU reactor the coolant and moderator are physical separated by virtue of the pressure and calandria tubes as can be seen in **Figure 2a**. Because of the physical separation, voiding of the coolant removes only a fraction of the heavy water within the lattice **Figure 2b**. The reactivity change induced by this loss of coolant is called the coolant void reactivity (CVR).

Specifically, the CVR, $\Delta\rho_{v-c}$, is the difference in reactivity between the voided, v, and cooled, c, states:

$$\Delta\rho_{v-c} \equiv \rho^v - \rho^c = \frac{1}{k^c} - \frac{1}{k^v} \quad (1)$$

In CANDU reactors the CVR is positive (Talebi 2006, Whitlock 1995). Meaning voiding of the coolant increases reactivity.

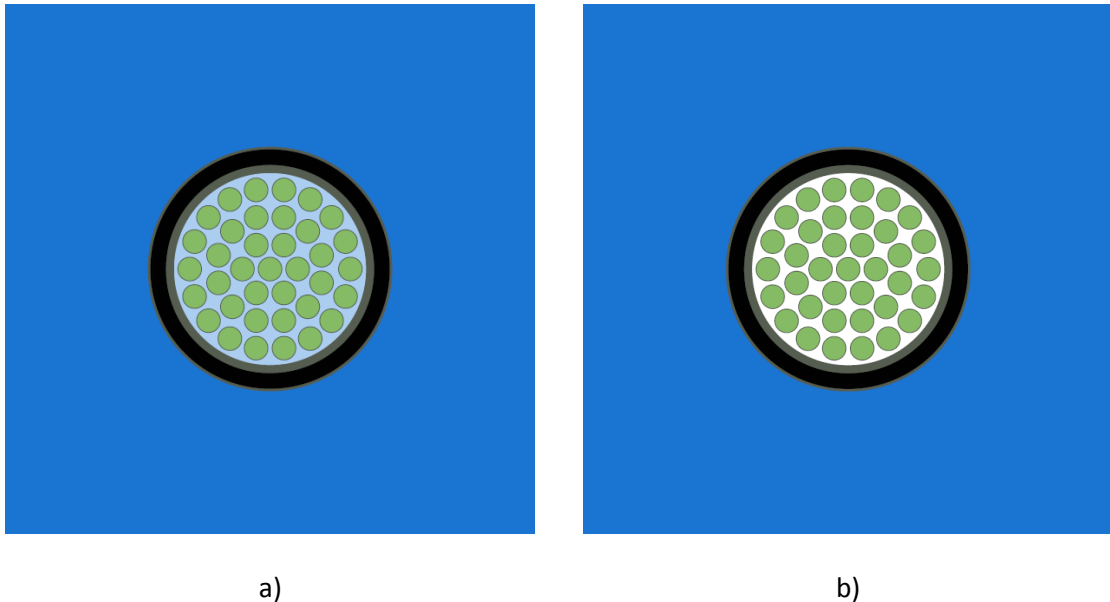


Figure 2 Typical CANDU6 lattice cell containing a 37-element fuel bundle in a) the cooled state and b) the voided state.

Comparison of **Figure 2a** and **Figure 2b** suggests the voiding of coolant only constitutes a partial loss of moderation. Moreover, it can be inferred from the result of a strongly positive coolant void reactivity in the CANDU lattice, that the partial loss of moderation from the absent coolant is not a dominant contributor to the net reactivity change.

As a thermal reactor, the CANDU relies on a moderator to slow fast fission neutrons to increase the likelihood those neutrons go on to induce further fissions within the fuel thus maintaining the chain reaction. As such, the effectiveness of the process, and by extension the reactivity, depends on how well:

1. Fast neutrons born in the fuel region migrate to the moderator to be thermalized and
2. Thermal neutrons from the moderator migrate back to the fuel region, remain thermal, **and** induce further fissions.

In the nominal cooled state, the coolant within the lattice impedes both these processes. Upon the coolant's removal the efficacy of both these processes is enhanced.

The net reactivity effect of voiding is the combination of several, at time competing, effects. These effects have already been itemized, quantified and separated into a series of spectral and spatial effects (Whitlock, 1995, Whitlock et al., 1995).

First, a minor component of the coolant void reactivity arises from the loss of material with a small but non-zero absorption cross-section within the lattice. Specifically, (Whitlock, 1995) has attributed approximately 0.3 mk of the CVR effect to the loss of absorption in coolant.

Next, the presence of the coolant in the fuel region provides a mechanism for down-scattering fast fission neutrons from the fuel to a lower energy where they are more likely to undergo non-productive resonance capture and less likely to cause fast fissions while they are still within the fuel region. Simultaneously, the comparatively hot coolant provides a mechanism for up-scattering thermal neutrons from the moderator. In each of these spectrum effects the presence of the coolant serves to hinder the generation of neutrons; conversely the coolants removal augments it.

For fuel that has accumulated plutonium through burnup there is a spectrum effect which dampens the coolant void reactivity. Plutonium, which is responsible for an appreciable portion of the fission neutrons generated in irradiated CANDU fuel in a cooled lattice, has a fission resonance at around 0.3 eV. As the spectrum changes in the fuel region when the coolant voids there are fewer neutrons whose energy corresponds to the plutonium resonance. Consequently, there are fewer plutonium fissions. In other words, the spectrum shift away from the plutonium resonance is a negative component of the coolant void reactivity.

Voiding of the coolant redistributes neutrons in energy within the fuel region and elsewhere. Voiding also redistributes neutrons spatially within the fuel region. The redistribution preferentially increases thermal flux in the inner rings of the fuel while decreasing flux in the outer ring. Epithermal flux decreases in all fuel rings but most in the inner rings. Finally, fast flux increases in all rings. The increase in fast flux in the fuel can be attributed largely to the decrease neutron down-scattering in the coolant within the pressure tube. A consequence of the general increase in fast flux within the

fuel is an increase in the fissions induced by fast neutrons. The increase in fast fission rate is another positive contributor to the coolant void reactivity.

The net result is a positive CVR on the order of +16 mk (Talebi, 2006) – well in excess of the delayed neutron fraction. Overall, the effect is tempered in CANDU reactors by a long neutron generation time when compared to other reactors (Muzumdar, 2009). Moreover, its potential impact is further accommodated by heat transport system loop(s) and shutdown system design. Nevertheless, in some situations or jurisdictions it may be considered desirable to reduce the coolant void reactivity.

The objective of this work is to assess the impact of adding moderator displacers to the CANDU lattice with respect to the coolant void reactivity with the intent of reducing it by changing the magnitude of the competing effects described above.

The document is structured as follows: Chapter II presents the general features of CANDU reactor CVR; Chapter III presents design options that have been used to reduce the CVR in CANDU and similar reactors; Chapter IV presents the methodology used to assess the CANDU lattice with close-packed displacers; Chapter V presents the effect of close-packed moderator displacers on the CANDU CVR; Chapter VI summarizes and makes general observations pertaining to moderator displacers in the CANDU lattice; and Chapter VII presents proposed future investigations.

Chapter II Features of CANDU Coolant Void Reactivity

This chapter summarizes the properties of the CANDU lattice germane to its CVR and will help understand some of the design options presented in subsequent chapters. The objective is to describe the problem that the displacers aim to address. Numerical results presented in this chapter are obtained using the transport code DRAGON (Marleau et al. 2007).

Moderator-to-Fuel Ratio:

In thermal reactors neutrons produced by the fission of fissionable isotopes have energies of the order of 1 MeV (Duderstadt, Hamilton, 1976), however, the neutrons that the reactor relies upon to induce those fissions have energies typically less than 1 eV. A moderator (light element) is used to slow fast neutrons to low (thermal) energies where they are more effective at inducing fissions. The efficacy of slowing fission neutrons depends, in part, on the amount of moderating material for a given amount of fuel; the moderator-to-fuel ratio. By extension the reactivity of the system also depends, in part, on the moderator-to-fuel ratio. This dependence for the fresh lattice is illustrated in **Figure 3** by changing the amount of moderator within a lattice either through changing the lattice pitch or the moderator density.

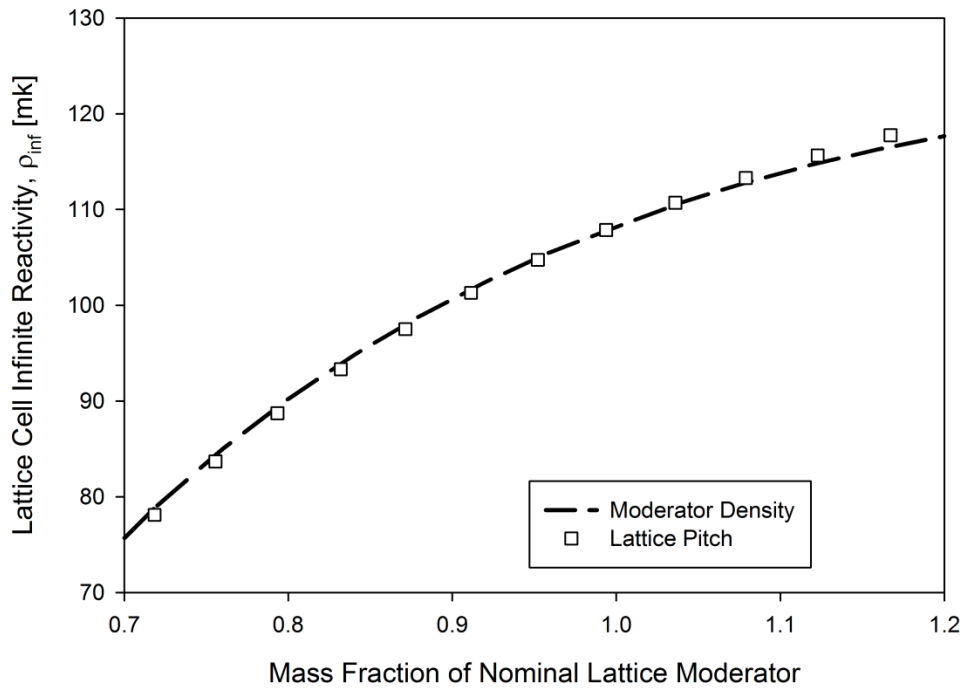


Figure 3 Reactivity dependence on the amount (mass) of moderator within the lattice cell.

Implicit in **Figure 3** is that only the moderator within a cell is changed and thus coolant is not considered to be a moderator in the figure. Also, for the sake of clarity, the fuel, pressure tube and calandria tube geometry remains unchanged in the simulations used to produce **Figure 3**. The coolant in CANDU reactors is distinct from the moderator and, as can be inferred from the positive CVR in the CANDU lattice, a decrease in the amount of coolant within the cell increases that cell's reactivity. In other words, the coolant-to-fuel ratio coefficient and the moderator-to-fuel ratio have opposite signs. Furthermore, the reactivity dependence of the moderator-to-fuel ratio is sensitive to the amount of coolant in the lattice cell, **Figure 4**.

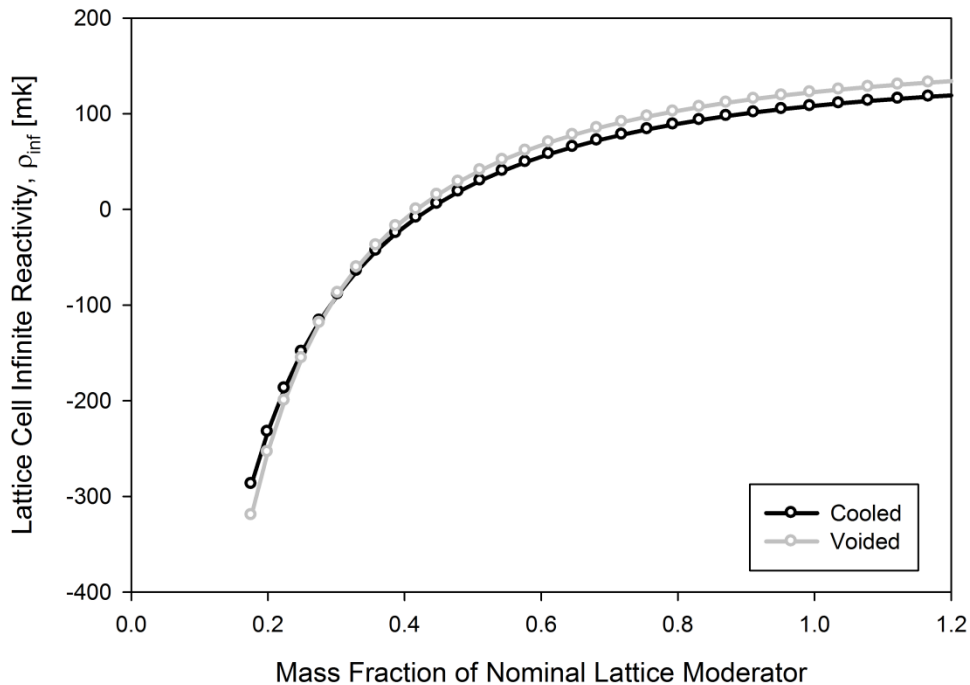


Figure 4 Comparison of the reactivity dependence on the amount (mass) of moderator within the fresh lattice cell between the cooled and voided cell.

What can be seen in **Figure 4** is that around the nominal amount of moderator (mass fraction of unity) the voided cell has a higher reactivity; a result consistent with a positive coolant void reactivity. However, there is a cross-over around 0.3 of the nominal amount of moderator within the cell. Below this point the voided cell is less reactive than the cooled cell. A lattice operating below the cross-over would have a negative coolant void reactivity.

If the exercise is repeated with a lattice containing irradiated fuel, specifically one corresponding to mid-burnup, the same cross-over is present again at around 0.30 of the nominal amount of moderator within the lattice cell; **Figure 5**. This suggests that the

cross-over location is not sensitive to burnup. However, it is apparent that the reactivity difference around the nominal moderator mass implies a value of CVR sensitive to burnup.

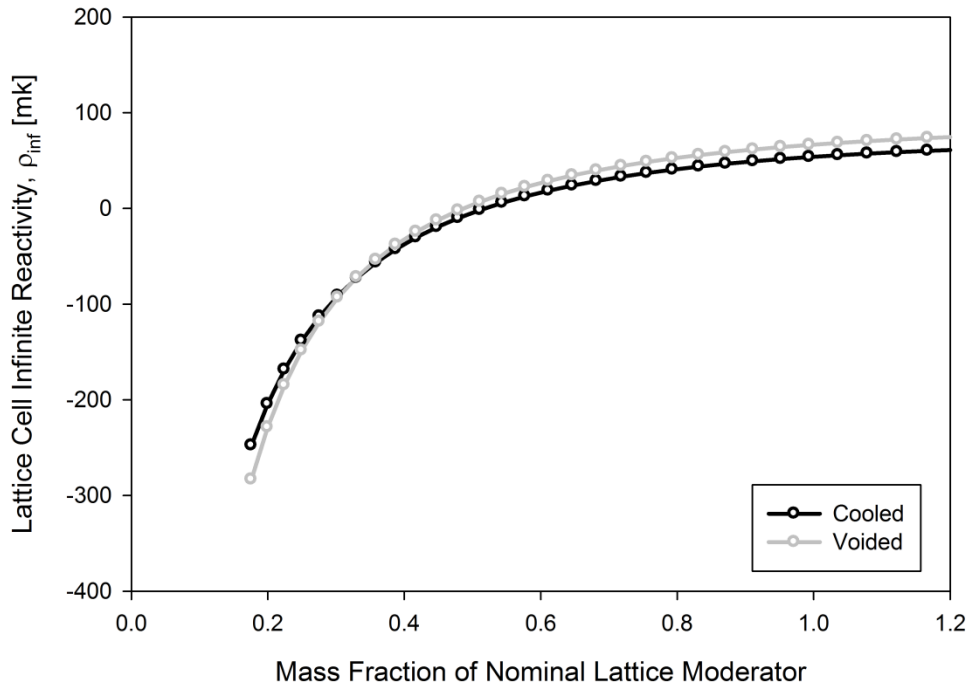


Figure 5 Comparison of the reactivity dependence on the amount (mass) of moderator within a mid-burnup lattice cell between the cooled and voided cell.

Burnup Sensitivity of CVR:

Comparison of **Figure 4** and **Figure 5** suggests a burnup dependence to the coolant void reactivity. Explicit plotting of the CVR with burnup for the nominal CANDU lattice in **Figure 6** confirms the burnup dependence.

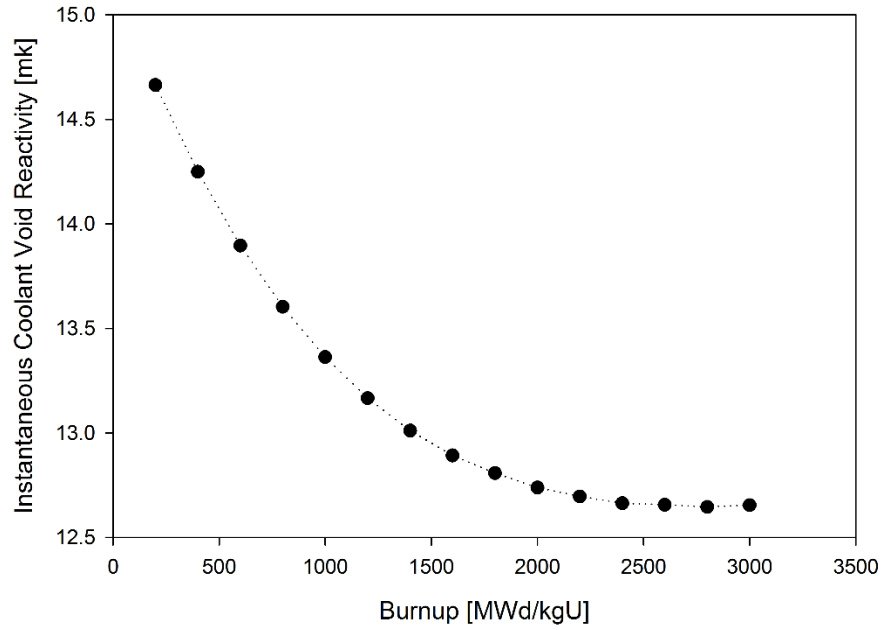


Figure 6 Coolant void reactivity as a function of burnup, presented from fresh to approximately mid-burnup fuel.

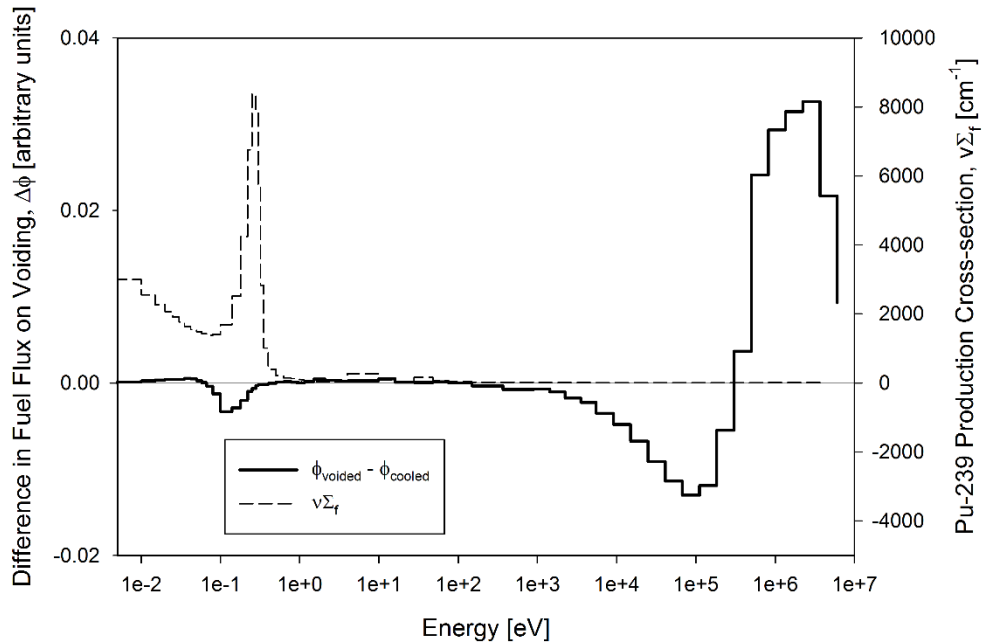


Figure 7 Change in fuel flux on voiding (solid) and the plutonium-239 production cross-section (dashed) with a resonance at approximately 0.3 eV.

According to (Whitlock, 1995) the burnup dependence of CVR stems from the accumulation of plutonium within the lattice. Specifically, plutonium exhibits a fission resonance at approximately 0.3 eV meanwhile the spectrum change upon voiding is such that there is a decrease in flux around that resonance, **Figure 7**, leading to fewer fissions from plutonium on voiding. The dependence of coolant void reactivity on the plutonium concentration highlights the importance of fuel composition to coolant void reactivity.

Spatial Dependence of Voiding:

Aside from differences in temperature, purity and density, the coolant and moderator are nearly identical materials. Even when these differences are removed by artificially assigning the coolant properties identical to those of the moderator, the calculated coolant void reactivity remains largely unchanged. This indicates that the thermal up-scattering component of the coolant void reactivity is small but, more importantly, that there is a significant spatial component. The spatial component is evident as removal of moderator outside the calandria tube, either through the reduction of lattice pitch or the moderator density results in a lower lattice cell reactivity yet the removal of the same material within the pressure tube (i.e. the coolant) results in an increased lattice cell reactivity. This implies that it is important whether the heavy-water is removed from within or outside the channel.

Reference (Whitlock, 1995) ascribes the spatial dependence to the loss of the primary scattering mechanism within the pressure tube. Furthermore, the loss of this scattering mechanism leads to a redistribution of the flux within the fuel. This redistribution can be visualized by taking the difference between the cooled flux and the voided flux. This difference, voided minus cooled, is presented for two energy groups in

Figure 8 and **Figure 9**. The difference in thermal flux, **Figure 8**, is such that the flux in the centre of the fuel increases upon voiding as described previously. Conversely, the difference in fast flux, **Figure 9**, is such that the neutron flux increases at the centre of the fuel. The flux in **Figure 9** differs from the previous description that portrayed the ‘fast flux’ increasing in every ring. The apparent disparity stems from a difference in the definition of fast flux. In **Figure 9** fast flux is defined as it traditionally is in the two-group case as any neutron whose energy is above 0.625 eV. The previous description however, described flux changes in three groups, thermal, epithermal and fast. According to that convention, **Figure 9** would be a combination of the epithermal and fast flux.

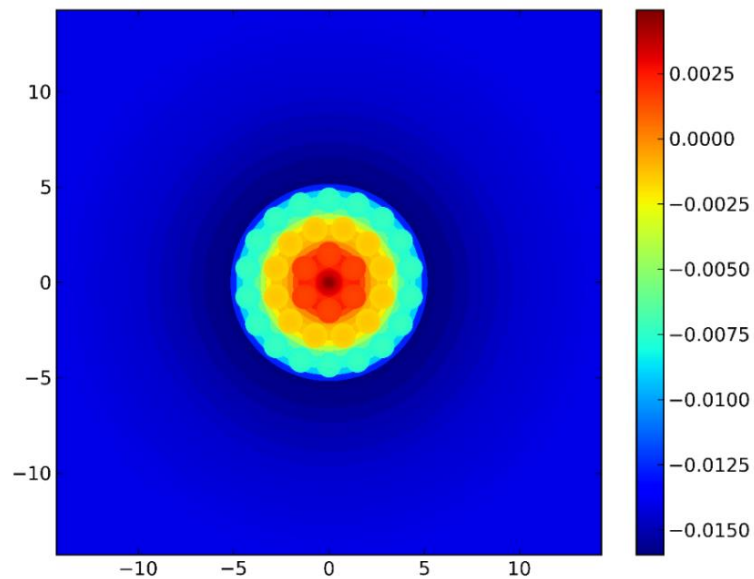


Figure 8 Difference (voided less cooled) in thermal (below 0.625 eV) flux within a fresh CANDU lattice (arbitrary units).

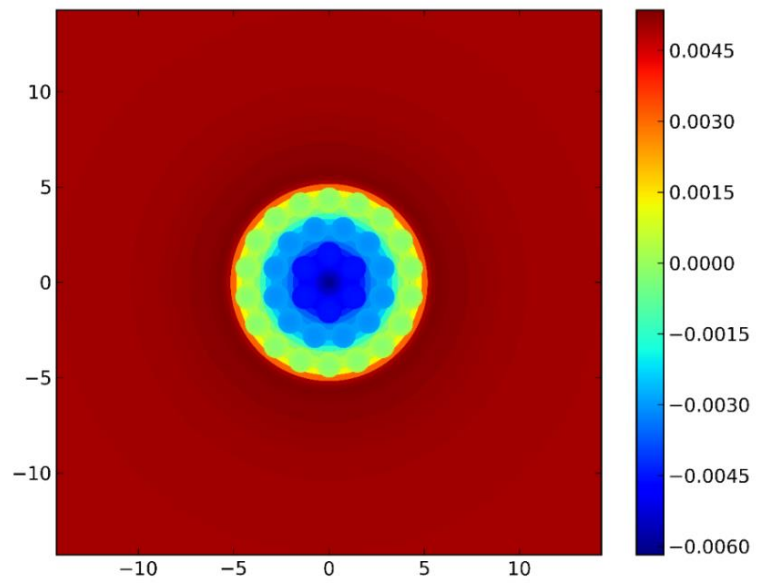


Figure 9 Difference (voided less cooled) in fast (above 0.625 eV) flux within a fresh CANDU lattice (arbitrary units).

Chapter III Review of Design Elements Intended to Manipulate Reactor Coolant Density Reactivity Coefficient

As discussed previously, it may be considered desirable to reduce the CVR of the CANDU lattice. This chapter presents some of the methods that have been put forward to date to reduce the CVR. For clarity all values, tables and figures in this literature review have been reproduced from the referenced material.

Steam Generating Heavy Water Reactor – Displacers Tubes:

The Steam Generating Heavy Water Reactor (SGHWR) concept was a pressure tube reactor heavy water reactor similar to the CANDU reactor. However, unlike the CANDU reactor, the design used vertical pressure tubes, a boiling light water coolant and enriched uranium fuel. A 104-channel 100 MWe prototype of the SCHWR was constructed at Winfrith and went online in 1967 (Pickman et al. 1979). The intent of the prototype was to serve as a proof of concept for subsequent higher power versions of the design (Rippon, 1974).

The prototype SGHWR control system was designed to accommodate a coolant void coefficient within a given range (Wray et al. 1968). To accommodate the uncertainty in the design predictions, which may have caused the physical reactor to have a coolant void coefficient outside of a tolerable range for the control system, a design element was included to make the coefficient tunable. A large set of displacer tubes ran parallel to the fuel channels, *Figure 10*. The displacers were organized into 11 gangs (or banks) (Hicks et al. 1968). In the event of an undesirably positive coolant void coefficient, the displacers could be drained by the gang to decrease the coefficient to

within a tolerable range. Conversely, in the event of an excessively negative void coefficient the light water impurity in the heavy water moderator could be increased to change the coefficient. In this way, the use of moderator displacers was instrumental for ensuring an acceptable coolant void coefficient in the SGHWR design by providing a mechanism to tune that coefficient. Ultimately, upon commissioning the reactor, however, the use of moderator displacers was determined to be unnecessary (Hicks, 1968).

Summarizing, although in the end the moderator displacer tubes in the prototype SGHWR design went unused they provide an example of the conscious inclusion of a design element specifically to adjust to coolant void reactivity in a reactor.

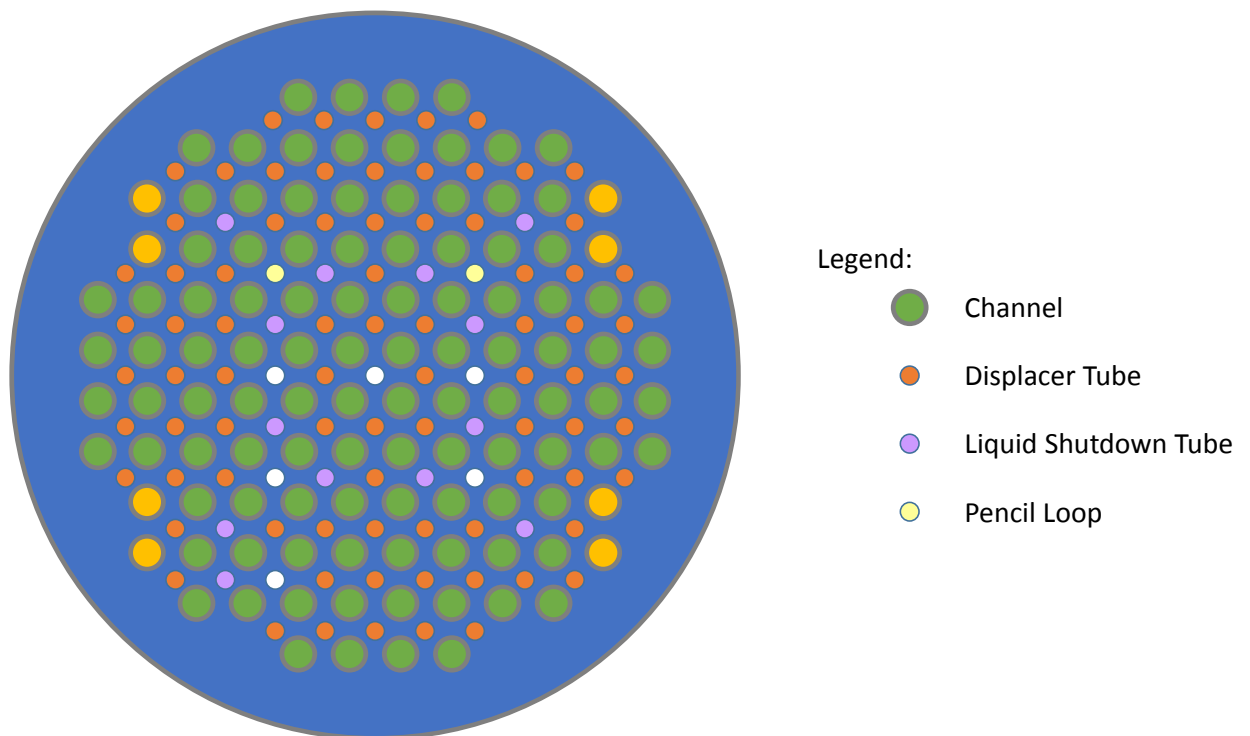


Figure 10 Core layout of the prototype SGHWR at Winfrith Hicks et al., (1968).

Moderator Displacers in Lattice Experiments:

Moderator displacers have also been the subject of experiments to ascertain their reactivity effect on the CANDU lattice (Green, 1968). The ZED-2 experiments summarized by (Green, 1968) displaced moderator with helium gas filled annular aluminum cans to simulate voiding as shown in **Figure 11**. These experiments concluded that the reactivity effect associated with the displacement was negative. The degree of reactivity change depended on the degree of moderator voiding and the axial location of the voiding.

Because the motivation for the experiments by (Green, 1968) was to investigate the effects of a moderator steam void resulting from the twin failure of the pressure tube and calandria tubes the study did not consider the impact on any of the lattice reactivity coefficients including the coolant void reactivity. Nevertheless, the result of displaced moderator leading to a decrease in reactivity is germane to the subject of this thesis and will be referred to in subsequent chapters.

Experiments in (Green, 1968) use a 19-element natural uranium bundle whose geometry is illustrated in **Figure 12 a** below. The differences in lattice geometry and composition notwithstanding, it is reasonable to expect that the sign of the reactivity change induced by moderator voiding is equally applicable to a 37-element fuel bundle.

Fuel-Bundle Design:

When the conscious effort to reduce the coolant void reactivity in CANDU reactors emerged in published documents, changes to the fuel were seen as a means to achieve a reduced coolant density coefficient while preserving much of the existing reactor design (Dastur, et al. 1990). Consequently, a series of new fuel bundle designs was proposed. The following paragraphs detail a selection of bundle designs intended to reduce the coolant void reactivity.

(Roshd et al. 1977) proposed changing the geometry of the fuel bundles to achieve a reduction in the coolant void reactivity. (Roshd et al. 1977) proposed to eliminate either the inner 7 elements of a 37-element bundle or the inner 19 elements of a 61-element bundle. The inner elements would be replaced with either a large un-voidable moderating element or simply void, **Figure 13**. (Roshd et al. 1977) recognized that the redistribution of flux within a bundle favoured the inner elements, **Figure 8**, while those same elements produced a disproportionately small fraction of the bundle's power during nominal operation. Therefore, eliminating the inner elements would diminish the positive reactivity effect of voiding while only slightly reducing the power the bundle could produce at nominal operation.

The bundle designs were evaluated by ZED-2 experiments and WIMS simulations. The results of these evaluations are summarized in **Table 1** which is reproduced from (Roshd et al. 1977).

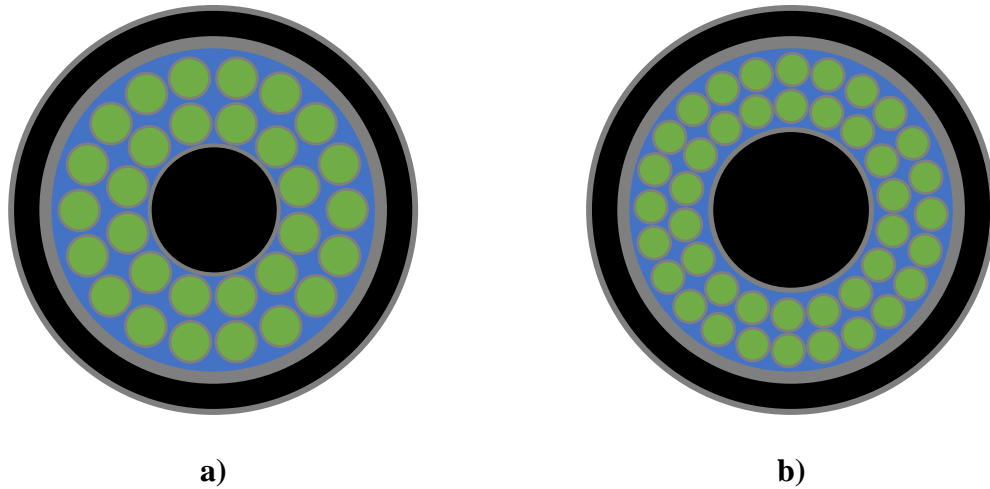


Figure 13 Bundle Geometries modified by eliminating the central elements to reduce coolant void reactivity. a) Modified 37-element bundle (with 30 elements) and b) modified 61-element bundle (with 42 elements); Roshd et al. (1977).

Table 1 Coolant Void Reactivity Reductions for Bundles Illustrated in Figure 13; Roshd et al. (1977)

	Void Reactivity Reduction (%)		Bundle Power Reduction (%)	
	Experiment	WIMS	Experiment	WIMS
Modified 37-element Geometry				
30-element void centre	41.9	43.3	12.7	12.2
30-element D ₂ O centre	39.8	35.9	12.2	11.6
Modified 61-element Geometry				
54-element void centre	27.5	29.3	-	5.5
42-element void centre	66.0	72.9	-	19.6
42-element D ₂ O centre	67.7	71.9	19.0	18.7

Alternatively, results produced by (Dastur and Buss, 1990) suggest it is possible to achieve a lattice void reactivity of zero without changing a 37-element bundle's geometry

through graded enrichment favouring the outer rings and a graded neutron absorber favouring the inner rings. Specifically, the simulations by (Dastur and Buss, 1990), suggest the enrichment and dysprosium grading summarized in **Table 2** would result in a lattice whose void reactivity was -4.1 mk at zero burnup increasing to -1.9 mk at mid-burnup and would achieve an exit burnup of 22 MWd/kgU with a 2.1 wt% average fuel enrichment.

Table 2 Intra-bundle Grading of Enrichment and Burnable Neutron Poison for Zero Void Reactivity Lattice; Dastur and Buss (1990)

	Ring 1	Ring 2	Ring 3	Ring 4
Fuel Enrichment (wt%)	1.1	1.1	3.37	2.03
Dysprosium Content (wt%)	9.08	9.08	0.0	0.0

The fuel design summarized in **Table 2** achieves a negative coolant void reactivity. The design exploits the redistribution of flux that occurs in the fuel upon voiding, **Figure 8**, whereby flux moves from more enriched fuel without poison in the outer rings to less enriched fuel with neutron absorbing dysprosium in the inner rings. The burnup consequence of introducing a neutron absorber is more than offset by the bundle's 2.1 wt% average U235 enrichment.

Dastur (Dastur et al. 1990) goes on to point out that the redistribution of flux upon voiding can be accentuated by changing the composition of the coolant as well as the fuel. Increasing the light water content during normal operation effectively shields the inner rings; the loss of that shielding upon voiding results in more pronounced redistribution of flux. Simulation results presented by Dastur and Buss 1990, and recreated in **Table 3**,

summarize the change in thermal neutron flux in a voided lattice for two coolant compositions:

Table 3 Influence of the Coolant Composition on the Thermal Flux within the Fuel on Voiding of the Coolant; Dastur and Buss, (1990)

Coolant Composition (Percent Light Water)	Percent Change in Thermal Neutron Flux in Fuel on Voiding			
	Ring 1	Ring 2	Ring 3	Ring 4
5%	+7.9	+9.7	+4.0	-2.9
15%	+24.4	+11.7	+5.0	-3.4

In effect, (Dastur and Buss, 1990) suggests the composition of the coolant could serve as a degree of freedom in the design of a lattice with a reduced coolant void reactivity. Tuning the redistribution of radial flux within the fuel on voiding results in a mechanism by which to adjust the importance of graded enrichment or graded poison concentration in the fuel rings.

In (Dastur et al. 1992) the work presented in (Dastur and Buss, 1990) was refined. Specifically, (Dastur et al. 1992) used expanded set of bundle geometries and described the role of depleted uranium in bundles that have been redesigned to reduce the coolant void reactivity in CANDU reactors. The premise was that the use of depleted uranium, effectively using U238 as an absorber, reduces the dysprosium needed to achieve a given void reactivity relative to (Dastur and Buss, 1990) bundle designs making void reduction more economical.

(Dastur et al. 1992) investigated two distinct bundle geometries: a standard 37-element fuel bundle and a 43-element bundle with a large centre pin. In both geometries

the two innermost rings are depleted uranium of 0.25 wt% enrichment. In the 37-element case both the central pin and the innermost ring are doped with dysprosium whereas in the 43-element bundle only the centre pin contains dysprosium owing to its large size. The remaining fuel is slightly enriched uranium whose U235 concentration depends on the dysprosium content of the inner rings which in turn depends on the desired coolant void reactivity. Both fuel geometries are shown in **Figure 14**.

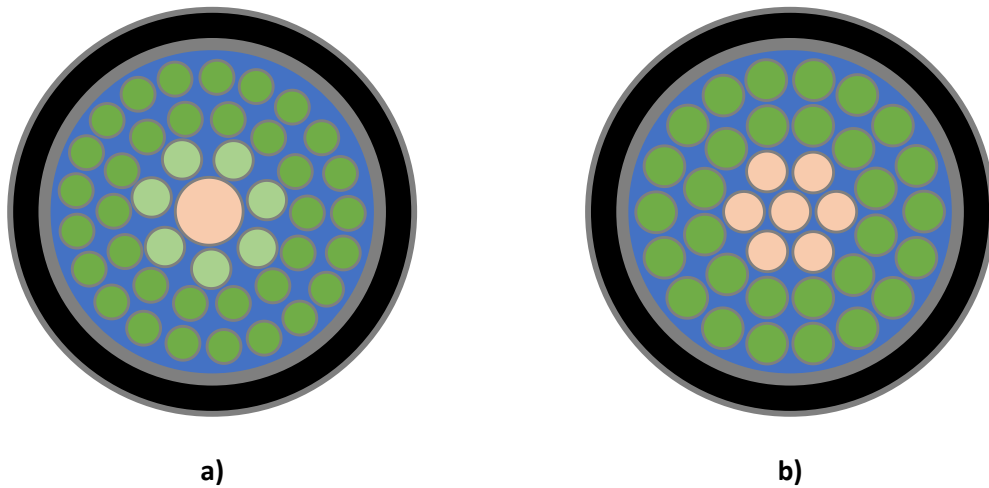


Figure 14 Comparison of bundle geometries a) 43-element bundle with large centre pin Dastur et al., (1992) b) standard 37-element bundle.

(Dastur et al., 1992) provides the results of a parametric study with differing dysprosium content in the centre element and the resultant coolant void reactivity for the 43-element geometry. Similarly, (Dastur et al., 1992) also provides the results of a parametric study where depleted uranium is not used in the inner elements of the 43-element bundle. Instead the effect of the dysprosium in the centre pin is offset by

uniform enrichment of the fuel. To facilitate comparison, the fuel enrichment was varied in each study such that the same burnup of 21 MWd/kgU was achieved in both cases.

Table 4 Parametric Study of Coolant Void Reactivity and Dysprosium Content in the Large Centre pin of a 43-element Bundle with Depleted Uranium in the Innermost Two Rings and Enriched Uranium in the Outermost Two Rings; Dastur et al., (1992)

Dysprosium Content (wt %)	Average Enrichment (wt%)	Enrichment in Outer Rings (wt%)	Coolant Void Reactivity (mk)
0.0	1.12	1.57	13.3
2.5	1.36	1.90	8.1
5.0	1.50	2.10	4.3
7.5	1.63	2.28	1.9
10.0	1.76	2.47	-0.4

Table 5 Parametric Study of Coolant Void Reactivity and Dysprosium Content in the Large Centre Pin of a 43-element Bundle with Uniformly Enriched Fuel; Dastur et al., (1992)

Dysprosium Content (wt %)	Average Enrichment (wt%)	Uniform Enrichment (wt%)	Coolant Void Reactivity (mk)
0.0	1.20	1.20	15.7
2.5	1.45	1.45	11.6
5.0	1.65	1.65	8.4
7.5	1.78	1.78	6.3
10.0	1.92	1.92	3.8

The comparison of the two 43-element bundle designs outlined in **Table 4** and **Table 5** in (Dastur et al., 1992) suggests that it is indeed more economical to achieve comparable reductions in void reactivity through the use of depleted uranium and burnable poison when compared to only using a burnable poison.

The early efforts redesigning the CANDU fuel bundle (Dastur and Buss, 1990; Dastur et al., 1992) culminated in AECL's Low Void Reactivity Fuel (LVRF) (Boczar et al., 1992). LVRF encompasses a variety of changes in the bundle design to reduce the value of the coolant void reactivity. The concept was initially conceived as an alternative fuel for CANDU reactors in foreign markets whose host countries may mandate a negative coolant void coefficient (Boczar and Sullivan, 2004). Subsequently, the design was also used as a basis for fuel design intended to burn actinides and dispose of plutonium (Chan et al., 1997).

The LVRF effort has an analogue in at least one other reactor. Atucha-II is a heavy water cooled and moderated Siemens designed reactor in Argentina (Ward et al., 2008). Notably, the reactor also has a positive void reactivity of approximately 10 mk (Ward et al., 2008). Similar to LVRF for the CANDU reactor, a conceptual fuel redesign has been studied for the Atucha-II reactor (Khatchikian and Fink, 2008). The results summarized by (Khatchikian and Fink, 2008) suggest that the approximately 10 mk CVR in Atucha-II can be reduced by approximately 5 mk using alternate fuels similar to LVRF.

Returning to CANDU fuel, among the design options discussed by (Whitlock, 1995), is a bundle that also incorporates an un-avoidable scattering material, not unlike the bundle design proposed by (Roshd et al., 1977). However, instead of the scattering

material belonging to a distinct fuel element (Whitlock, 1995) considers the case where each fuel element in a 37-element bundle is either accompanied by a graphite core or surrounded by a graphite annulus **Figure 15**.

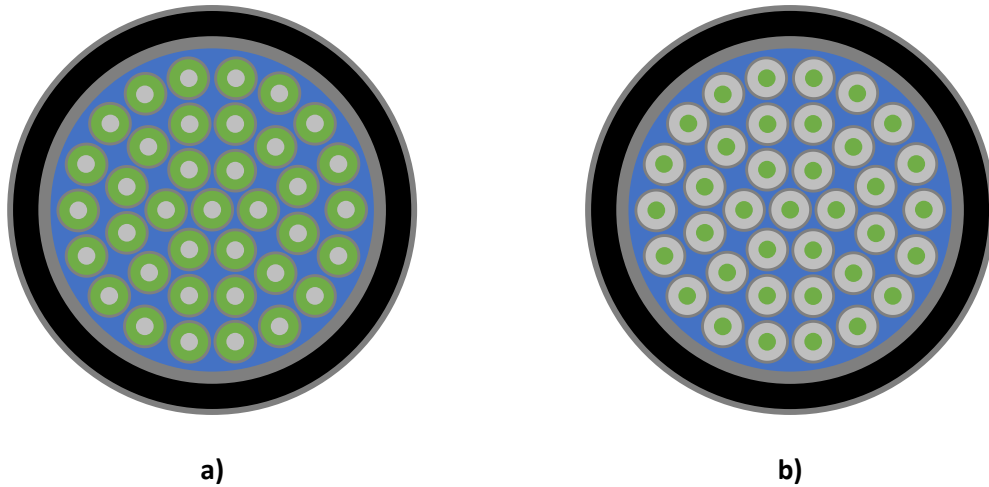


Figure 15 Standard 37-element bundle with elements a) having a graphite core and b) being surrounded by a graphite annulus; based on Whitlock, (1995)

For each of the fuel bundles pictured in **Figure 15** (Whitlock, 1995) considered two cases. First, considering the case where the uranium remained at its natural isotopic concentration. Next, considering the case where the uranium enrichment was such that the number of U235 atoms was conserved between the reference bundle and the bundle with graphite occupying some volume of the element. The results obtained by Whitlock for each bundle are summarized in **Table 6** and **Table 7** below.

**Table 6 Effect of Graphite Core within the Elements of a 37-element bundle;
Whitlock (1995)**

Volume Fraction of Graphite (%)	Graphite Core Diameter (cm)	Natural Uranium Case	U235 Conserved Case
		CVR (mk)	CVR (mk)
0.0	0.0	16.3	-
10.8	0.2	16.0	14.9
43.4	0.4	15.0	10.7
67.7	0.5	13.6	7.2

**Table 7 Effect of Graphite Annulus around the Elements of a 37-element bundle;
Whitlock (1995)**

Volume Fraction of Graphite (%)	Graphite Annulus Thickness (cm)	Natural Uranium Case	U235 Conserved Case
		CVR (mk)	CVR (mk)
0.0	0.0	16.3	-
10.8	0.0337	15.8	14.7
43.4	0.1505	14.2	10.3
67.7	0.2623	13.5	7.0

It can be seen from **Table 6** and **Table 7** that the graphite annulus surrounding the fuel elements gives slightly better results; (Whitlock, 1995) reasons that this is because when graphite on the exterior the uranium does not shield the scattering material (i.e. the graphite).

Departing further from traditional CANDU bundle design, (Whitlock, 1995) also puts forward an annular fuel bundle as a means of reducing the coolant void reactivity.

Instead of rings of discrete fuel elements, the bundle is comprised of three concentric nested natural UO₂ fuel tubes surrounding a central graphite spacer. The bundle's fuel annuli allow coolant to flow between them **Figure 16**.

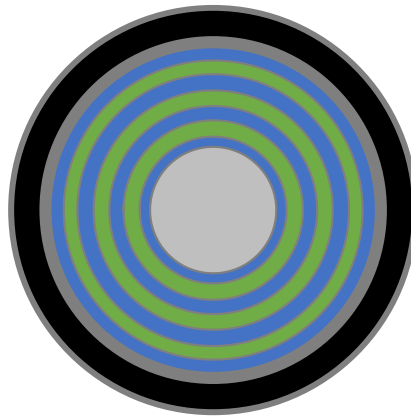


Figure 16 Annular fuel bundle Whitlock, (1995).

The natural UO₂ annular fuel put forward by (Whitlock, 1995) as pictured in **Figure 16** achieved a marked reduction in the coolant void reactivity. Whitlock calculated the coolant void reactivity of the zero burnup and mid-burnup lattice cell to be 7.2 mk and 2.9 mk respectively. Having only 68% of the fuel mass of the 37-element fuel bundle the fuel utilization decreased to 6.5 MWd/kgU compared to the 37-element bundle's 7.5 MWd/kgU according to (Whitlock, 1995).

(Whitlock, 1995) also explored the effects of using non-uranium fuel to reduce void reactivity. Whitlock recognized that the lattice coolant void reactivity decreases with irradiation due to the accumulation of plutonium. Consequently, as plutonium is present from the outset in mixed oxide (MOX) fuels, a CANDU bundle whose MOX fuel

has the same plutonium composition as in the outer rings of a typical CANDU bundle at discharge achieves a 4 mk reduction in CVR for a 1 wt% mixture. Whitlock indicates diminishing returns in terms of coolant void reactivity with increasing plutonium weight fraction.

Many of the fuel bundle designs that have been discussed by (Whitlock, 1995) as well as the design by (Roshd et al., 1977) have featured un-voidable scattering elements to offset the loss of scattering in the absence of the coolant in a voided cell. Meanwhile, (Dastur and Buss, 1990; Dastur et al., 1992) has proposed modification of the material in the central elements of standard bundle geometries. Combining these philosophies, (Min et al., 1995) proposes replacing the depleted uranium and the poisoned depleted uranium in (Dastur and Buss, 1990; Dastur et al., 1992) with graphite and poisoned graphite for the inner elements of the fuel bundle. (Min et al., 1995) uses WIMS calculations to compare both a standard 37-element bundle and a 43-element bundle with large centre element with graphite and dysprosium inner rings to the corresponding bundles with depleted uranium and dysprosium in the inner rings – in each case the outer rings of the fuel are enriched to 1.2 wt% U235.

It is worth noting that most of the analysis regarding the effects of fuel changes on coolant void reactivity has been performed at the lattice level often with the transport code WIMS. The lattice approach will be the approach used for analyses presented in this thesis using the transport code DRAGON.

Table 8 Comparison of a 37-element Bundle with Depleted Uranium and Dysprosium Inner Rings and Graphite and Dysprosium Inner Element; Min et al., (1995)

Dysprosium Content (wt%)	Discharge Burnup (MWd/kgU)			Mid-burnup Coolant Void Reactivity (mk)		Energy Output by Bundle (MWd)	
	DU		Graphite	DU	Graphite	DU	Graphite
	all rings	rings 3&4					
0	15.907	18.287	20.336	11.5	9.7	295.9	286.7
10	5.386	6.561	17.173	2.3	8.3	100.2	242.1
20	4.524	5.520	12.520	2.0	3.2	84.1	176.5
25	-	-	10.515	-	1.9	-	148.3
30	-	-	9.403	-	1.4	-	132.6
40	3.966	4.826	8.300	1.9	1.0	73.8	117.0
100	3.378	4.056	6.529	1.5	1.5	62.8	93.5

Table 9 Comparison of a 43-element Bundle with Large Centre Pin with Depleted Uranium and Dysprosium Inner Rings and Graphite and Dysprosium Inner Element Min et al., (1995)

Dysprosium Content (wt%)	Discharge Burnup (MWd/kgU)			Mid-burnup Coolant Void Reactivity (mk)		Energy Output by Bundle (MWd)	
	DU		Graphite	DU	Graphite	DU	Graphite
	all rings	rings 3&4					
0	16.127	18.412	20.360	11.6	9.9	296.1	287.1
1	10.569	12.439	-	6.6	-	194.0	-
1.5	6.469	7.803	-	2.4	-	118.8	-
2	3.196	3.926	-	0.6	-	58.7	-
5	0.188	0.234	16.357	-0.7	8.3	3.5	230.6
7	-	-	14.153	-	5.9	-	199.6
8	-	-	12.721	-	4.3	-	179.4
9	-	-	10.929	-	2.5	-	154.1
10	-	-	9.022	-	0.9	-	127.2
11	-	-	7.463	-	0.1	-	105.2
12	-	-	6.297	-	-0.7	-	88.8

Core Design:

Thus far retrofits to existing reactors have been discussed. However, in the interim new reactor designs have emerged. A new design provides the opportunity to include features to reduce the coolant void reactivity from the outset.

Notable designs include the advanced CANDU reactors: the ACR-700 (Ovanes and Chan, 2002) and the ACR-1000 (Buijs et al., 2008). More recently, a pressure tube

super critical heavy water reactor (PT-SCWR) is being considered as a possible contributor to the next generation of reactors (Pencer and Colton, 2013). Both reactor designs, the ACR and the PT-SCWR, were intended to have a negative coolant void reactivity and achieved it in a similar but subtly different way. Primarily, two effects were used in concert to reduce the coolant void reactivity of the designs.

First, the moderator to fuel ratio was reduced. The reduction was realized by decreasing the distance between adjacent channels, decreasing the lattice pitch, and increasing the calandria tube outer radius with respect to the traditional CANDU design. Specifically, the ACR-700 features a 22.0 cm lattice pitch (Cotton et al., 2005), the ACR-1000 features a 24.0 cm lattice pitch (Buijs et al., 2008) and the PT-SCWR features a 25.0 cm lattice pitch. Both values (of the lattice pitch) are markedly smaller than the 28.6 cm CANDU lattice pitch. Simultaneously, the calandria tube outer radius for the advanced CANDU reactors measures approximately 7.8 cm while the pressure-tube outer radius for the PT-SCWR measures approximately 9.1 cm for the 78-element PT-SCWR, both larger than the 6.6-cm traditional CANDU calandria tube outer radius. The modifications relative to the traditional design combine to effectively reduce the amount of moderator in a lattice cell which in both reactors contains a mass of fuel comparable to that in the regular CANDU lattice cell. As an illustration a scale comparison of the traditional CANDU lattice to the 78-element PT-SCWR lattice appears in **Figure 17** below.

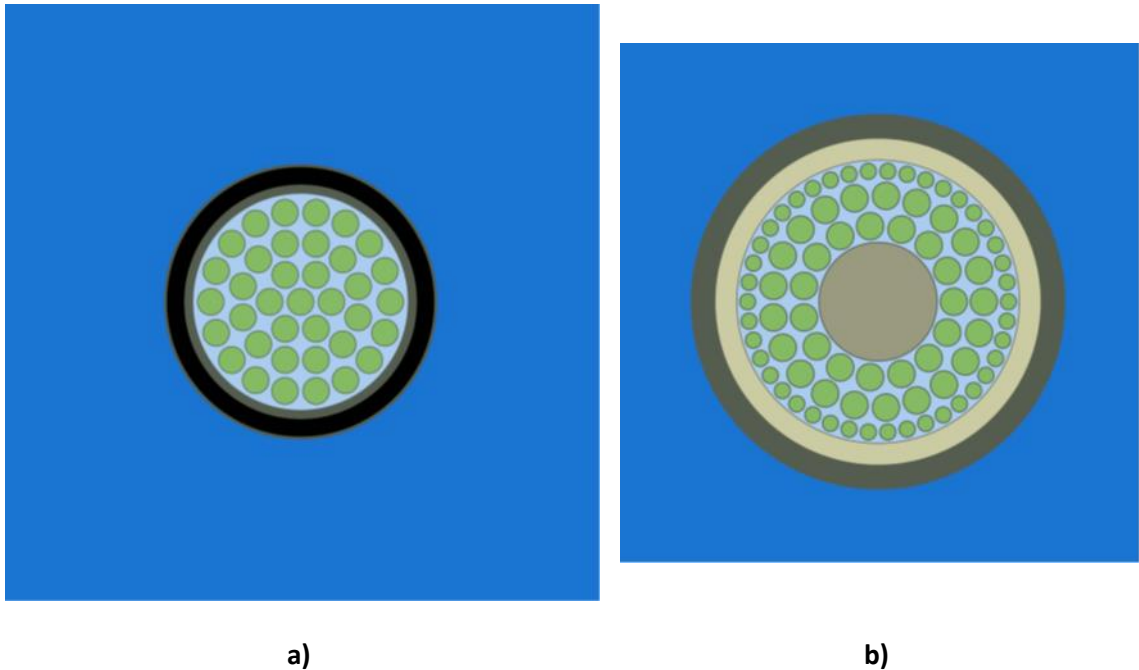


Figure 17 Scale comparison of a) the traditional 37-element CANDU lattice and b) the 78-element PT-SCWR lattice based on (Farkas and Nichita, 2014).

The second mechanism, used in tandem with the reduced moderator-to-fuel ratio, is the fuel design. The ACR-700 and ACR-1000 use slightly enriched uranium fuel; enriched uranium has long been considered in new and existing CANDU reactors (Bonalumi, et al., 1980; MacGillivray et al., 1986; Boczar et al., 1987; Chan and Dastur, 1987). On the other hand, the 78-element PT-SCWR uses a plutonium-thorium fuel. A common element between the fuel designs, however, is the use of a non-fuel central element. The advanced CANDU reactors use a central pin with burnable neutron absorbers whereas the PT-SCWR uses a large non-fuel zirconia element; **Figure 17b**. In each case the non-fuel central elements have been included to diminish the coolant void reactivity effect by taking advantage of the redistribution of flux within the fuel upon voiding.

In summary, the two primary measures for reducing the coolant void reactivity in the advanced CANDU reactor and the 78-element PT-SCWR designs are reducing the moderator to fuel ratio and a fuel bundle that takes advantage of the redistributed flux within the fuel upon voiding.

Chapter IV Methodology and Modelling Considerations

As introduced in the preceding chapters the focus of this thesis is the use of moderator displacers to reduce the coolant void reactivity in the CANDU lattice cell. Specifically, the intent is to use close packing of spherical displacers to reduce the amount of moderator volume within a simulated lattice cell to increase the relative importance of the coolant as a moderator resulting in a favourable re-balancing of the components itemized in Chapter 1. Moreover, the aim of the work is to investigate a means of reducing the coolant void reactivity that could theoretically be applied to existing CANDU reactors where the core geometry is fixed. The proposed displacers would surround CANDU fuel channels outside the calandria tubes as illustrated in **Figure 18**.

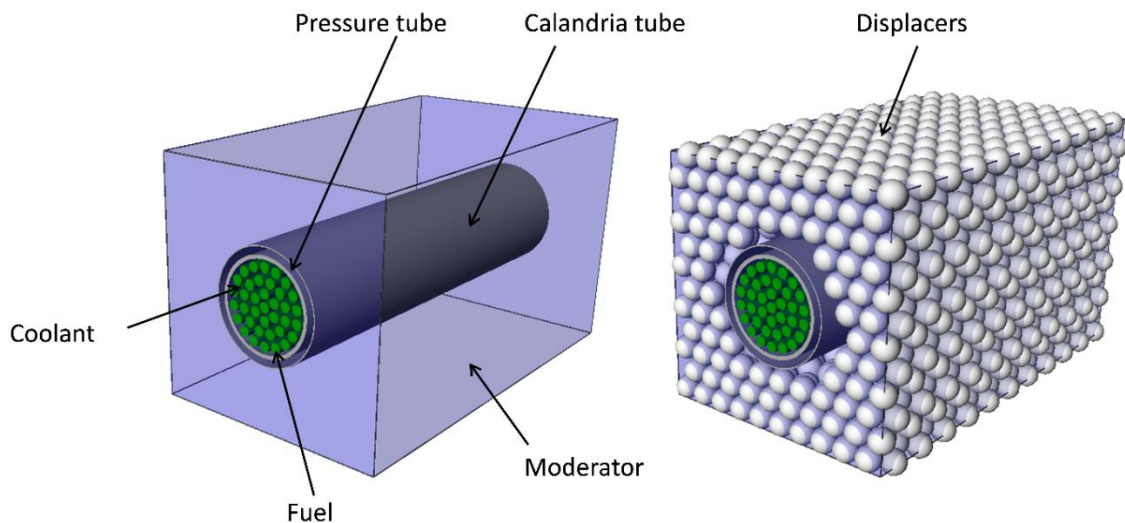


Figure 18 Three-dimensional lattice cell (a) without displacers and (b) with displacers.

The displacers illustrated in **Figure 18** would be able to displace a maximum of approximately 74% (or exactly $\frac{\pi}{3\sqrt{2}}$) of the moderator in the limit of small displacers.

The displacement is sufficient to lower the amount of moderator within the cell below the cross-over point in **Figure 4** and **Figure 5**.

Since the sole purpose of the displacers is to reduce moderation by occupying space that would otherwise be filled with heavy-water, they should, ideally, not interact at all with neutrons, thus not contributing to either neutron slowing down or absorption. Parasitic slowing-down in the displacers would reduce or negate their effectiveness in reducing moderation while parasitic absorption would unduly reduce the achievable burnup. To minimize neutron interaction with displacer material, this study proposes the use of hollow spheres since, from a neutronic perspective, a shell with vanishingly small thickness would be ideal. From a mechanical perspective, however, the feasibility of a displacer shell will also depend on its strength. So, in practice, the displacer shells will occupy some finite volume within each lattice cell, depending on their thickness.

Given that any non-ideal displacer will interact with neutrons depending on its thickness to an extent governed by the materials neutronic properties, much of this work takes the form of scoping studies investigating the impact of these two degrees of freedom; thickness and material.

Continuous Fuelling Approximation:

The results presented below use lattice calculations to assess the impact of varying the thickness and materials of the close-packed moderator displacers. Consequently, it is necessary to arrive at a framework to extend the lattice results such that they are

representative of full-core behaviour. The continuous refuelling homogeneous model provides that framework.

CANDU reactors are fuelled on-power during normal operation. Fresh bundles are added at one end of the fuel string while spent bundles are discharged at the other. In this way a small fraction of the fuel is replaced nearly continuously. As a result of the nearly constant refuelling, after a sufficiently long period of normal operation, the core reaches a state whereby it contains bundles with a burnup distribution from nearly fresh to burnups exceeding the average exit burnup. This state is referred to as the equilibrium core (Rozon, 1991). As refuelling continues, individual-bundle properties change considerably (as a function of individual-bundle burnup) but the overall characteristics of the (equilibrium) core, like reactivity, change little.

An accurate determination of the equilibrium core reactivity requires detailed knowledge of the instantaneous burnup distribution in the core as well as of the exact position of the reactivity devices. A useful simplification is the continuous refuelling approximation (Rozon, 1991), which makes the following assumptions:

1. Refuelling of each channel is continuous, the fuel being pushed in at a constant speed,
2. For each channel, the refuelling speed is adjusted such that the discharge fluence (also called discharge irradiation) has the same value over large burnup regions. The core can have one or more such burnup regions, and
3. The burnup in the true reactor flux can be approximated by the burnup in a single-cell with reflective boundary conditions.

The continuous-refuelling approximation leads to the Continuous-Refuelling Homogeneous Model (Rozon, 1991), in which the refueling-region-average few-group macroscopic cross sections are calculated as averages over the length of a fuel channel, which translate into averages over irradiation. For a reactor with a single burnup region, the approximate cross sections of the equilibrium core are calculated, according to the homogeneous model, as:

$$\hat{\Sigma}_g^{core}(\omega^{disch}) = \frac{\int_0^{\omega^{disch}} \hat{\Sigma}_g(\omega) d\omega}{\omega^{disch}} \quad (2)$$

In the above, the hat represents cell-homogenization and group condensation and

$\omega = \int_0^t {}^{SC} \hat{\Psi}(\tau) d\tau$ is the cell irradiation (fluence). ${}^{SC} \Psi$ represents the two-dimensional

flux in a lattice cell as obtained from a single-cell calculation. The infinite-lattice multiplication constant corresponding to average core properties can subsequently be calculated based on the average cross sections provided by the homogeneous model. In the two-group approximation, and for a single refueling region encompassing the entire core, the formula is:

$$k_{\infty}(\omega^{disch}) = \frac{\hat{\Sigma}_{f1}^{core}(\omega^{disch}) \left[\hat{\Sigma}_{s1 \rightarrow 2}^{core}(\omega^{disch}) + \hat{\Sigma}_{a2}^{core}(\omega^{disch}) \right] + \nu \hat{\Sigma}_{f2}^{core}(\omega^{disch}) \hat{\Sigma}_{s1 \rightarrow 2}^{core}(\omega^{disch})}{\hat{\Sigma}_{a2}^{core}(\omega^{disch}) \left[\hat{\Sigma}_{a2}^{core}(\omega^{disch}) + \hat{\Sigma}_{s2 \rightarrow 1}^{core}(\omega^{disch}) \right] + \hat{\Sigma}_{s1 \rightarrow 2}^{core}(\omega^{disch}) \hat{\Sigma}_{a2}^{core}(\omega^{disch})} \quad (3)$$

Assuming the leakage and absorption due to reactivity devices and structural materials to be approximately equal in the cooled and voided cases, the equilibrium core CVR for a given discharge irradiation can be expressed as:

$$\Delta\rho_{v-c}^{equil}(\omega^{disch}) = \left[\frac{1}{k_{\infty}^c(\omega^{disch})} - \frac{1}{k_{\infty}^v(\omega^{disch})} \right] \quad (4)$$

In the above, letters c and v denote the cooled and voided states respectively.

Lattice Model:

The lattice calculations are performed using the deterministic lattice code DRAGON (Marleau et al., 2007) – specifically version 3.05E. DRAGON has been selected as it is a freely available (i.e. non-proprietary, no license required) code capable of performing both the transport and burnup calculation in a reasonable amount of time. An example of a DRAGON input file taken from (Marleau et al., 2007) and is included in Appendix A.

For the calculations described below DRAGON uses the collision probabilities method to solve the transport equation within a cell. DRAGON is also able to solve the depletion equations and to produce the fuel compositions at discrete burnup steps as the simulated fuel burns. These features are applied to a standard lattice model used in the moderator displacer assessment.

The lattice model itself is two-dimensional with reflective boundary conditions. The transport calculations are performed in 69 energy groups using nuclear data from the IAEA WIMS-D formatted WLUP library (Leszczynski, et al. 2007). **Figure 19** below gives an indication of the geometry used in the lattice cell calculations to model the

nominal lattice, **Figure 19a**, and the displaced lattice, **Figure 19b**. An indication of the spatial discretization over which properties (e.g. flux, material composition etc.) are assumed uniform is also provided in the figure. Also noteworthy, as an assumption, the fuel temperature is assumed to be uniform across all fuel regions. Similarly, the coolant density and temperature is uniform across the coolant regions and is invariant over the burnup range; this translates to assuming coolant density and temperature to be invariant axially along the channel. This departs from the physical case where coolant properties vary axially along the channel from inlet to outlet and bundles will burn in the local conditions as opposed to the assumed ones. Related to the above assumption, the use of the term ‘cooled’ in this work refers to the lattice state where coolant is present within the pressure tube at its nominal density and is not intended to suggest the absence of boiling within the channel. Nonetheless, the assumptions are standard simplifications in reactor lattice calculations.

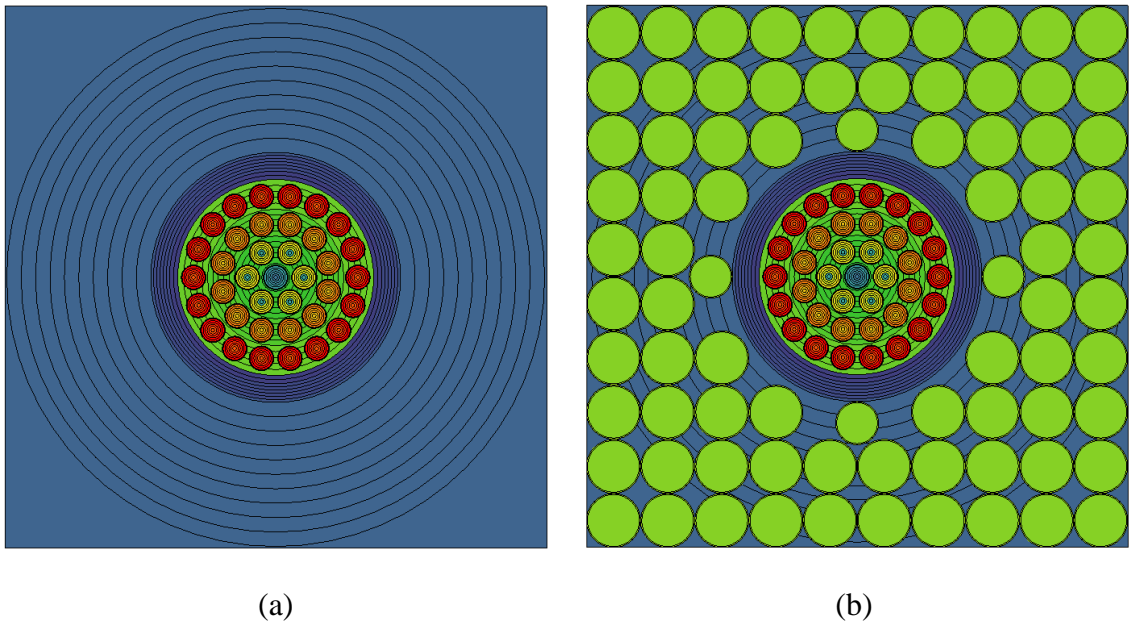


Figure 19 DRAGON models of (a) a typical CANDU lattice and (b) a CANDU lattice cell with displacers.

A primary DRAGON calculation burns the fuel in cooled configuration in the presence of the displacers to a simulated burnup of 5.2×10^4 MWd/T over the course of 91 burnup steps. At each of these steps the cell-homogenized two-group lattice cross-sections are generated for use in the continuous-refuelling homogeneous model (Eq. (2)). A secondary set of DRAGON calculations then uses fuel compositions at each of the 91 burnup steps obtained from primary DRAGON calculation to again solve the transport equation except now in the voided state to produce the corresponding cell-homogenized two-group lattice cross-sections. This process is illustrated for the 91 burnup steps in **Figure 20** below.

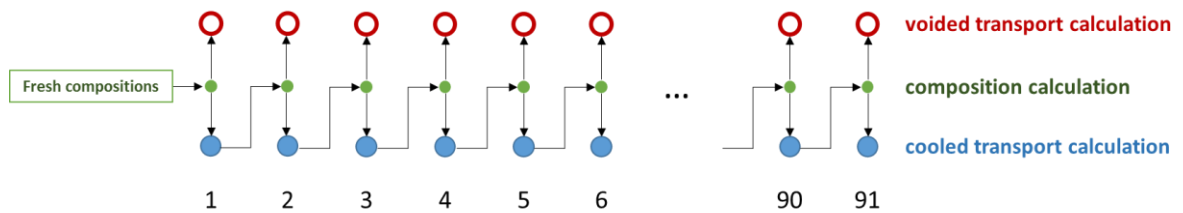


Figure 20 Graphical summary of the calculation methodology.

To represent a three-dimensional array of displacers in a two-dimensional model, the HCP spheres are represented as a square array of annular displacers **Figure 19b**. For the retrofitted two-dimensional lattice to maintain equivalence with the three-dimensional model, the inner and outer annulus radii are set to such values as to reproduce the fractional volume of heavy-water, air and sphere material in the true three-dimensional configuration. To satisfy the fractional volume condition and to accommodate the presence of the calandria tube, two sizes of annuli are used.

The annular displacers are positioned initially in a 10×10 uniform square array that covers the entire lattice cell. The outer radius of the annuli is chosen so that the

annuli touch each other and thus cover 78.54% of the entire cell area, a fraction slightly larger than the desired 74.05%. The resulting outer radius is $r_o = 1.429$ cm. The annuli overlapping the fuel channel are subsequently removed and an additional four, smaller, annuli are added in the moderator region to achieve a moderator-only displacement fraction exactly equal to 74.05%, which corresponds to the three-dimensional HCP configuration. The four slightly-smaller displacers are positioned at the compass points around the calandria tube and have an outer radius $r_o = 1.138$ cm, determined from the condition that exactly 74.05% of the entire cell moderator be displaced.

For each annulus, regardless of its outer radius, the inner radius is calculated so that the fractional area occupied by its “skin” is the same as the volume fraction occupied

by the wall of the corresponding hollow sphere, that is $\frac{\text{annulus } r_i^2}{\text{annulus } r_o^2} = \frac{\text{sphere } r_i^3}{\text{sphere } r_o^3}$.

Implicit in the assumption of equivalence between the two-dimensional and three-dimensional lattice cell is the assumption that similar moderator-to-coolant ratios yield similar CVR values regardless of the method used to change the amount of moderator. To evaluate this assumption, burnup averaged CVR values were calculated for a lattice with 2.0 wt% enriched fuel¹ and ideal zero-thickness displacers using three separate methods of reducing the amount (i.e. total mass) of moderator within the lattice cell: decreasing the lattice pitch, artificially reducing the moderator density and using displacers. Results are shown in **Figure 21**, which shows agreement between the CVR values obtained using the three different methods of varying the amount of moderator in

¹ Enriched fuel was used so that the cell would have meaningful burnup over which to calculate burnup-averaged properties.

the cell. The agreement in **Figure 21** suggests the CVR is not sensitive to the means of reducing the amount of moderator in the regions outside the calandria tube and, consequently, that the two-dimensional annular displacers are a suitable surrogate for the spherical ones in three dimensions. In particular, agreement between the CVR values obtained using the two-dimensional model with displacers and those obtained using reduced-density moderator (which can be thought of as corresponding to uniformly-distributed infinitely-small displacers) suggests that the detailed distribution of the displacers is also not important and therefore that the slight irregularity introduced by the use of the four small displacers immediately adjacent to the calandria tube does not substantially influence the computed CVR values.

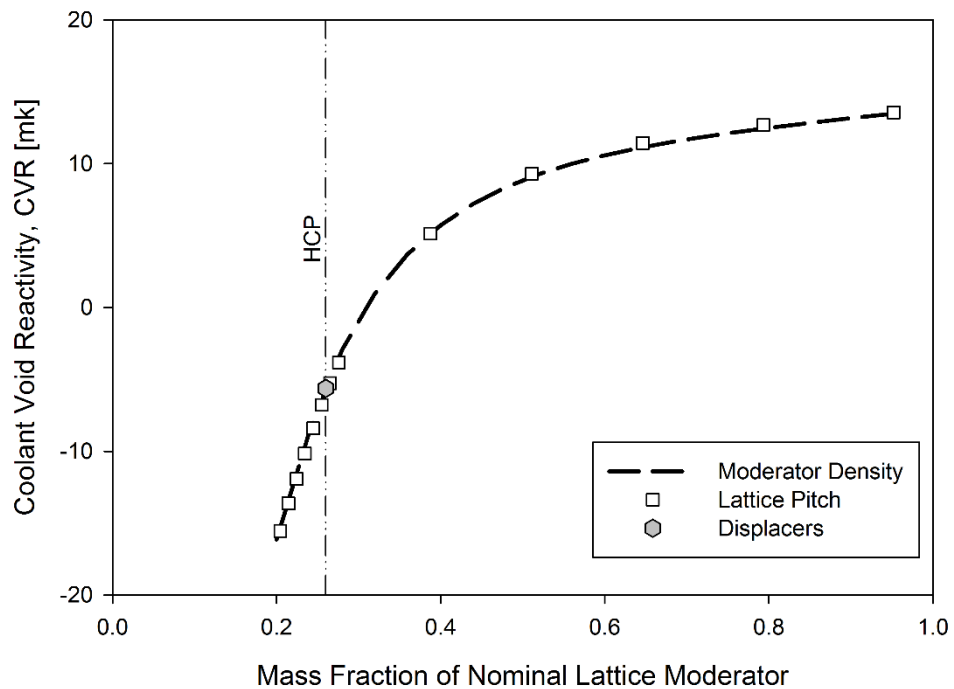


Figure 21 Comparison of mechanisms for reducing CVR (2.0 wt% fuel enrichment; 0.00 cm displacer thickness).

To be able to average properties to their discharge burnup according to the continuous fuelling approximation it is important to quantify the value of the discharge burnup. The discharge burnup can be determined from the condition that the equilibrium-core be critical, that is its reactivity be zero. Because an infinite-lattice model does not account for leakage or the presence of additional absorbers (e.g. reactivity devices which are not present in the simple lattice model in **Figure 19** but that would be present in the reactor core that is being represented), the corresponding equilibrium infinite-lattice reactivity has a small positive value. For the purpose of this work, that value is determined by applying Eq. (2) to the “regular” CANDU lattice, for which the nominal discharge burnup is known to be approximately 7500 kWd/kgU (Nichita, 2008). The corresponding equilibrium infinite-lattice reactivity is found to be approximately 52 mk, as seen from **Figure 22**. Consequently, when the burnup averaged reactivity in a displaced lattice reaches 52 mk it is considered to have reached its discharge burnup.

Extending the 52 mk average reactivity criterion from the nominal lattice to the lattice with displacers carries with it the assumption that device reactivity worths and leakage (which account for the 52 mk supercriticality of the bare, infinite lattice) do not change with the introduction of displacers and the attendant change in spectrum.. Adjuster rod reactivity worth has been shown to change in response to changes in fuel type (Kim, Suk, 2002)² and it is likely that the leakage will also change in response to the addition of displacers into the reactor’s moderator. Nonetheless, the changes are expected to be small enough as to be negligible. A rudimentary indication of the sensitivity to

² Undoubtedly some of the change is due to a change in neutron spectrum induced by the alternate fuel in (Kim, Suk, 2002).

change in the 52 mk criterion for discharge burnup due to the introduction of displacers can be drawn from the slope of the burnup-average reactivity near the presumed discharge burnup suggesting the sensitivity to be approximately 150 kWd/kgUmk. The impact in terms of discharge burnup is small compared to the discharge burnups observed even for errors of several mk of reactivity. It would then follow that sensitivity of burnup averaged coolant void reactivity to the integrated reactivity discharge burnup criterion is moderate as well.

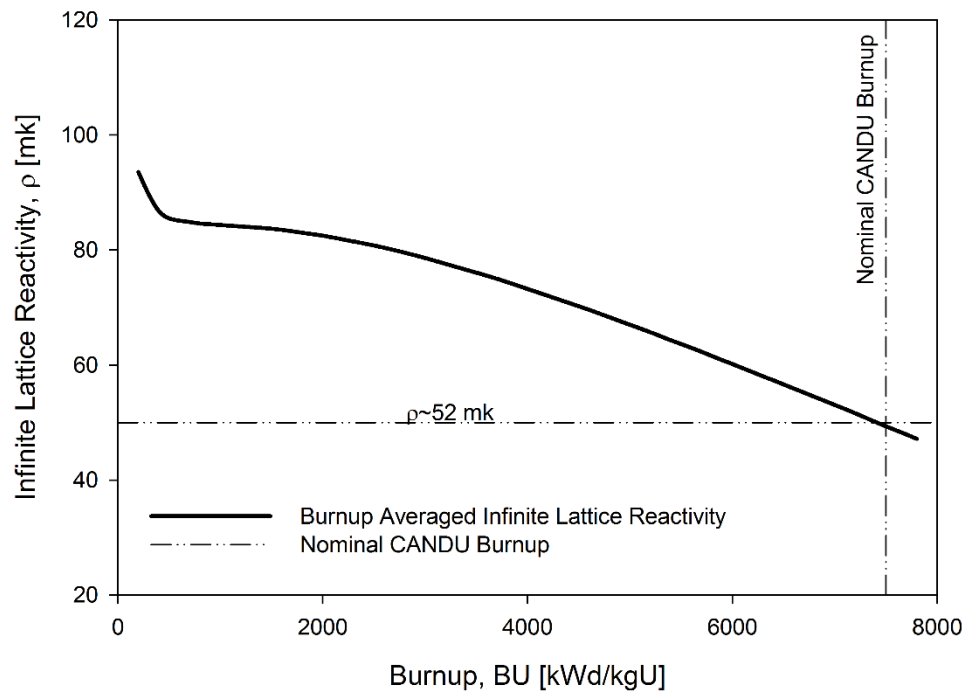


Figure 22 Burnup averaged reactivity curve for the nominal CANDU lattice.

Displacer Material Selection:

The displacer shell materials considered in the scoping studies are: zirconium, graphite, beryllium, lead and aluminum. The materials are chosen primarily for their low neutron absorption as itemized in *Table 10*³. Two of the materials, graphite and beryllium, can even be considered moderating materials characterized by their low absorption cross-section, high scattering cross-section and low atomic weight. Other displacer materials were initially considered but excluded from further analysis. For example stainless steel, while having attractive mechanical and corrosion properties, has comparatively higher neutron absorption and a core using 0.01-cm thick stainless-steel displacers was found to be still slightly sub-critical for 4%-enriched fresh fuel. For this reason, stainless steel displacers were excluded from further consideration.

Table 10 Macroscopic Cross-sections and Atomic Weights for 2200 m/s neutrons for Select Materials (ANL-5800, 1963)

	Atomic Weight	Absorption, Σ_a (cm ⁻¹)	Scattering, Σ_s (cm ⁻¹)	Total, Σ_t (cm ⁻¹)
D ₂ O	20.030 (2.0 for D)	3.3×10^{-5}	0.449	0.449
Zirconium	91.22	0.008	0.338	0.347
Graphite	12.011	32×10^{-5}	0.385	0.385
Beryllium	9.013	124×10^{-5}	0.865	0.865
Lead	207.21	0.006	0.363	0.369
Aluminum	26.98	0.015	0.084	0.184

³ To facilitate comparison to the heavy water the shells are displacing D₂O cross-sections also appear in *Table 10*.

Displacer Thickness:

Five sphere thickness values are investigated for each material: 0.01 cm through 0.05 cm in increments of 0.01 cm. As previously established, thinner spheres are preferable from a neutronic perspective. The 0.01 cm lower limit is assumed in this work to be achievable from a manufacturing perspective and to also provide sufficient resistance to buckling.

As a cursory exploration of the resistance to buckling, the following formula can be used to estimate the buckling pressure for a spherical shell (Carlson, et. al., 1967)

$$P_c = \frac{2E}{\sqrt{3(1-\nu^2)}} \left(\frac{t}{R} \right)^2 \quad (4)$$

where E is Young's modulus, ν is the Poisson ratio, t is the shell thickness and R is the outer radius. The resulting buckling-pressure values for a 0.01 cm thickness and different materials⁴ are shown in **Table II** for displacer radii corresponding to that pictured in **Figure 19b**. For each material considered the buckling pressure is above the hydrostatic pressure corresponding to a 10 m column of water. Because the horizontal calandria vessel is approximately 6m in diameter, it stands to reason that a 0.01 cm thickness would withstand the resulting hydrostatic pressure. To allow for any aberrations, for example the actual buckling pressure being lower due to manufacturing imperfections and to

⁴ The buckling pressure for graphite is not presented due to the non-availability of suitable Young's modulus data.

pressure concentration at the points where spheres touch each other, thicker shells, up to 0.05 cm, are also considered. Ultimately, the final choice of shell thickness will have to be based on more detailed neutronic and mechanical calculations beyond the scope of this work. Finally, it is noteworthy that due to buoyancy, the resulting force on thin-walled displacers will be directed upwards and, in the case of lead, a 0.05 cm wall thickness corresponds to nearly neutral buoyancy.

Table 11 Buckling Pressure for Select Materials

Material	p_c [MPa] ($t = 0.01$ cm)
Zirconium	5.2
Graphite	-
Beryllium	16.2
Lead	1.0
Aluminum	4.2

Uniform Fuel Enrichment:

As demonstrated by Green (1968), displacement of the moderator reduces the reactivity of the CANDU lattice. Compounding the reactivity reduction from the reduced moderation within the lattice cell due to the spherical displacers is the introduction of absorption in the displacer material itself. The reduction in reactivity translates to a reduction in discharge burnup. Uniform fuel enrichment is used to compensate for the reduction in core reactivity caused by the displacers and by doing so recover a practicable discharge burnup.

For all materials, fuel enrichments of up to 4% are considered, corresponding to typical enrichment values for LWR fuel. The lower limit of the studied enrichment interval is dependent on material and is usually chosen so that the achievable burnup at the lowest studied enrichment is not far below the 7500 kWd/kgU value corresponding to natural-uranium-fuelled CANDU reactors.

General Methodology:

Having established the means to determine the discharge burnup and the burnup averaged CVR for a given combination of displacer material, uniform fuel enrichment and displacer thickness, and, having established a reasonable set of values for each of these parameters it is straightforward to arrive at a method to assess each combination of values. That method is captured in the flowchart illustrated in *Figure 23*.

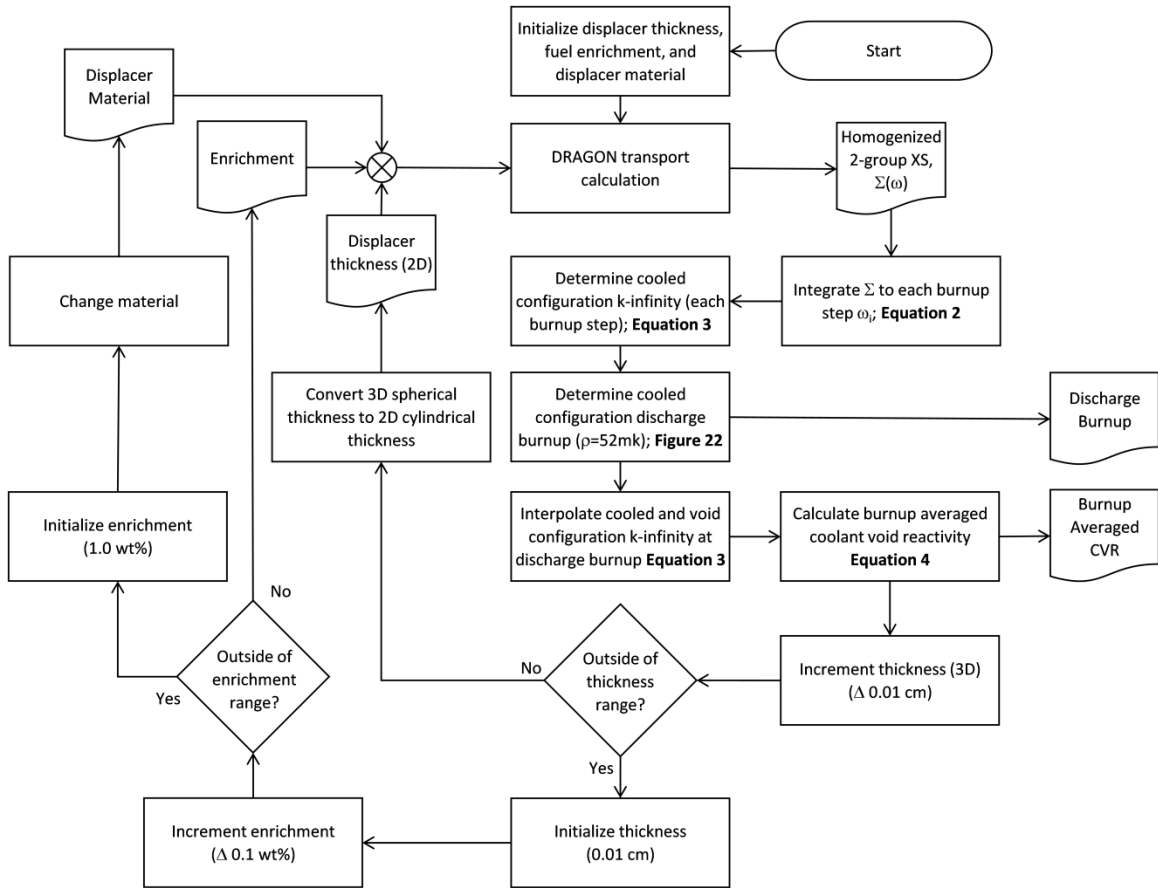


Figure 23 Flowchart depicting the scoping study methodology.

Chapter V Close-Packed Moderator Displacers

The results presented below take the form of scoping studies: the CVR and achievable discharge burnup are calculated for different displacer materials and different sphere wall thicknesses at different fuel enrichment values.

No Material (zero thickness) Results:

For completeness, although corresponding to no material in particular, zero shell thickness results were also generated and are included along with each material's results to show how far finite-thickness results differ from the neutronic ideal case. For

clarity it is worth noting that the zero-thickness results are identical for all materials as material composition is irrelevant for vanishingly-thin spheres.

The zero-thickness displacer case also provides a material independent point of comparison to the traditional un-retrofitted lattice. As such, before discussing the retrofitted lattice with finite sized displacer shells, it is appropriate to make a comparison of the spectrum between the retrofitted and nominal lattices. That comparison is presented in **Figure 24** below. Evident in **Figure 24** is that, as expected, in the case of the retrofitted lattice there is a decrease in the number of thermal neutrons on voiding ostensibly due to the increased importance of the coolant as a moderator.

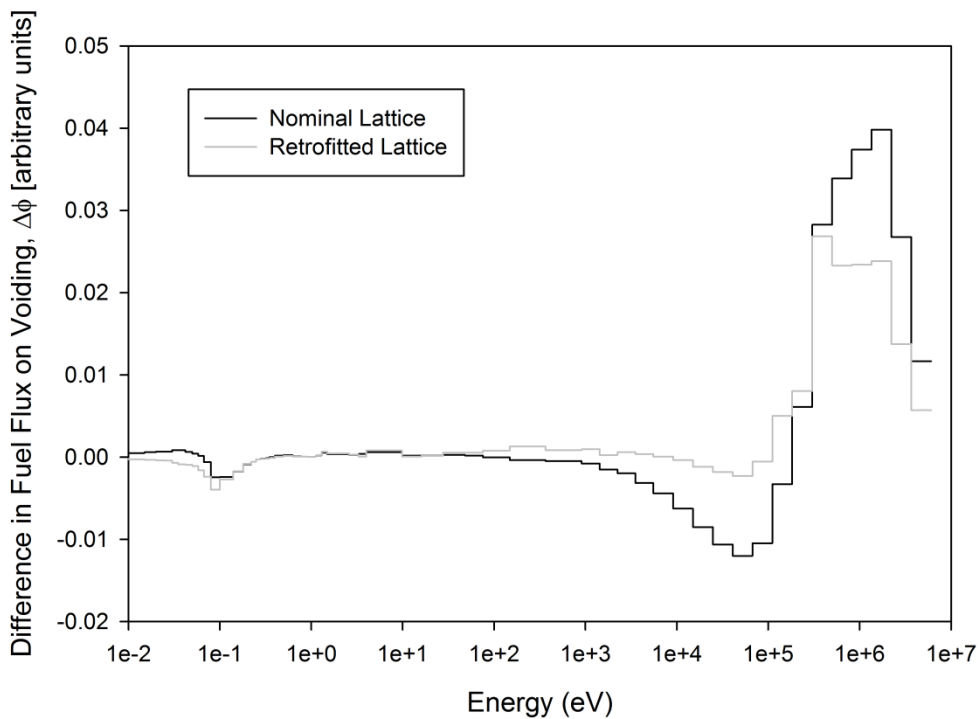


Figure 24 Change in fuel flux on voiding for both the fresh nominal (black) and fresh lattice with displacers (grey).

Zirconium:

The first displacer material considered is zirconium. The material is identical to the calandria tube composition assumed in the lattice model used in the assessment outlined in this work. Because zirconium is already used for lattice components in the un-modified lattice there exists a logical precedent for its expanded use in the modified lattice.

In terms of the thickness-enrichment scoping study results for each displacer thickness considered, the burnup averaged CVR values are presented in **Figure 25** and the projected discharge-burnup results are presented in **Figure 26**.

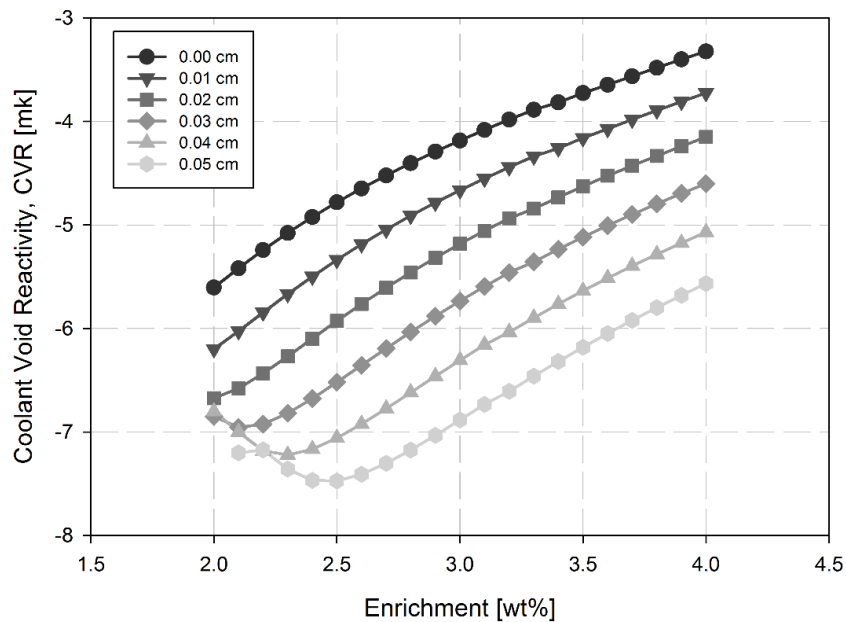


Figure 25 Burnup averaged coolant void reactivity for zirconium displacers.

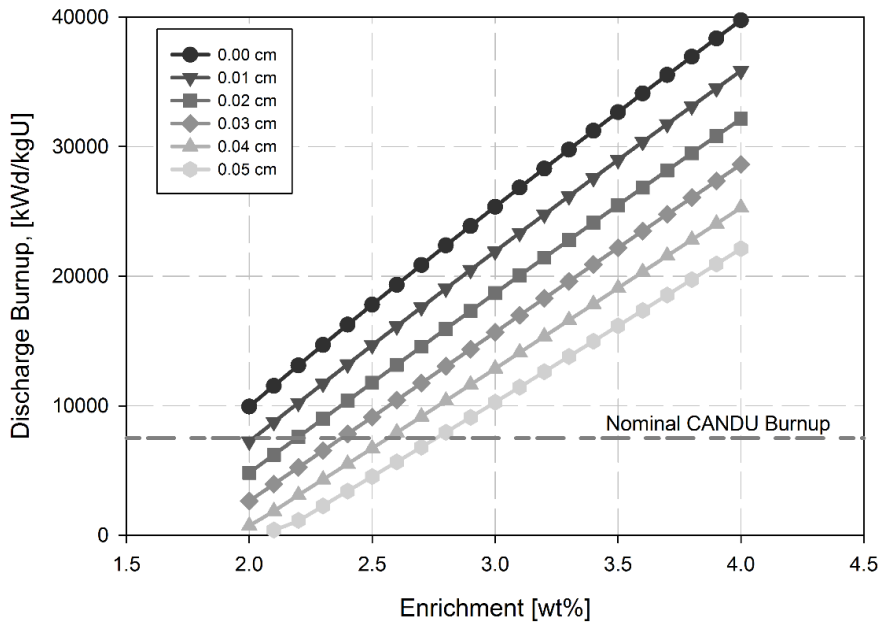


Figure 26 Discharge burnup for zirconium displacers.

It can be seen that zirconium displacers exhibit a negative CVR for all values of the sphere thickness considered. Generally, in the case of zirconium displacers, the CVR is reduced (i.e. becomes more negative) as the shell thickness increases due to increased absorption in the displacer material upon voiding reducing the reactivity of the voided case as discussed in detail below.

The CVR also increases with enrichment. While a detailed analysis of CVR components is beyond the scope of this work, it will be noted that the observed increase in CVR with enrichment is consistent with the presence of a low-lying Pu resonance which has a negative contribution to the CVR when the fuel spectrum changes due to the loss of coolant. As fuel is enriched, the fraction of fissions occurring in Pu decreases and hence the negative CVR component decreases, leading to an increase in the CVR. As this

effect is independent of the displacer material or thickness it is observable in the remainder of the scoping studies.

Figure 26 shows that for zirconium displacers the negative burnup averaged CVR comes with a penalty in the discharge burnup. As shell thickness increases so too does non-productive neutron absorption within the shell material. In the case of zirconium displacers, an enrichment of approximately 2.0 wt% is necessary to maintain the nominal 7500 kWd/kgU CANDU discharge burnup for the thinnest studied shell (0.01 cm) and around 2.7 wt% is required to maintain CANDU discharge burnup for the thickest shell (0.05 cm).

Graphite:

The next displacer material considered is graphite. Unlike zirconium, graphite is not currently used extensively within the components of a traditional CANDU lattice. Nevertheless, it has been considered for use in the fuel (Min et al., 1995) and has been used extensively in other reactor designs as a moderator (Baker, 1970). As such, graphite does have considerable pedigree as an in-core reactor material and thus is considered as displacer material in this scoping study without making claim to its suitability for this purpose from a mechanical standpoint.

The results for graphite differ from zirconium in terms of both the burnup averaged CVR and the achievable discharge burnup **Figure 27** and **Figure 28**. Firstly, graphite displacers provide a more modest reduction in the CVR when compared to

zirconium displacers, and because the trend of increasing CVR with increasing enrichment remains common these effects conspire to produce a positive CVR for the thickest displacers considered (0.05 cm), for high enrichments. However, the trend observed for zirconium displacers of decreasing CVR for increasing shell thickness is reversed in the case of graphite displacers. Secondly, the discharge burnups achieved with the graphite displacers are greater than those for the zirconium displacers. Also, it can be seen that the zirconium displacer trend of decreasing discharge burnup with increasing shell thickness is reversed in the case of graphite displacers. For graphite displacers, reclaiming the traditional CANDU burnup for the thinnest considered shell (0.01 cm) is done with an enrichment of less than 1.8 wt% (compared with around 2.0 wt% in the case of zirconium displacers) and for the thickest considered shell (0.05 cm) the enrichment required to reclaim the traditional CANDU burnup decreases to around 1.6 wt% (compared to 2.7 wt% for zirconium displacers).

Many of the effects observed for graphite displacers, specifically, the more modest reduction in CVR when compared to zirconium displacers, the opposing trend in thickness versus CVR and the opposing trend in discharge burnup versus thickness can be attributed to the fact that graphite is itself a moderator. Thus, unlike the addition of zirconium to the lattice, the addition of graphite to the lattice serves to re-introduce the moderation the displacers were intended to remove. This is not to say that this makes graphite displacers undesirable as they still serve to reduce the CVR while requiring less fuel enrichment to recover typical CANDU fuel utilization values.

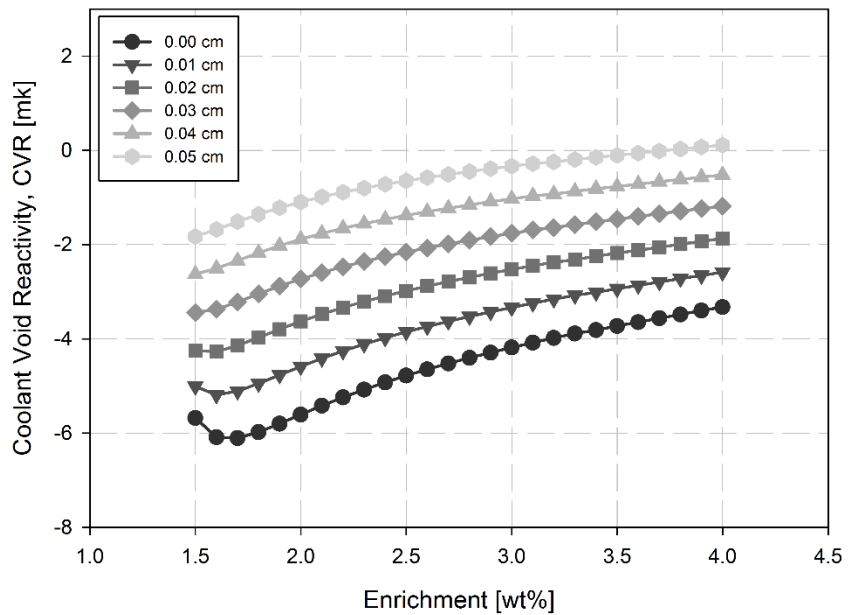


Figure 27 Burnup averaged coolant void reactivity for graphite displacers.

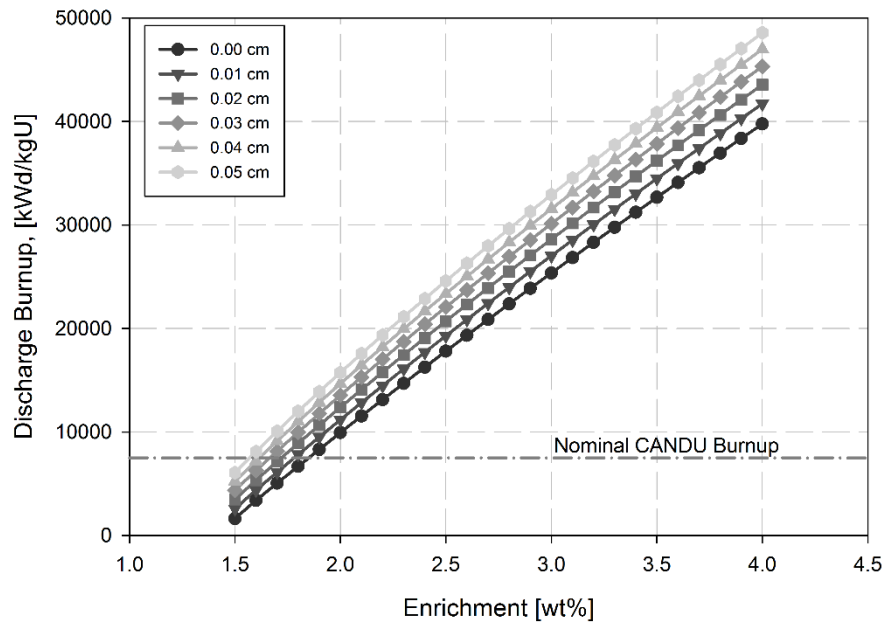


Figure 28 Discharge burnup for graphite displacers.

Beryllium:

Similar to graphite, the next material considered, beryllium, is also a moderator except to an even greater extent. Beryllium also has the advantage of a history as a material used in nuclear applications; particularly as a good moderator (Beeston, 1970). Its widespread use is limited in part by its cost and toxicity (Lang, 1994). Notwithstanding these limitations, the beryllium is considered here for the scoping studies outlined.

It is apparent from the burnup averaged CVR, **Figure 29**, and discharge burnup, **Figure 30**, results that the primary difference between graphite and beryllium is the degree of moderation re-introduced to the cell for corresponding shell thicknesses. Notably, for beryllium displacers, any shell thickness exceeding 0.02 cm the simulation results ensures a positive value for the burnup averaged CVR, whereas for graphite displacers positive CVR values were only observed for the thickest displacers studied (0.05 cm) and even then only for the highest enrichments considered (greater than 3.6 wt%). Also, as would be expected from a material that is a better moderator, the discharge burnup has increased markedly over that obtained with graphite. Indeed, for higher enrichment values for the thickest displacers considered the discharge burnup values exceeded the simulated burnup range with a maximum limit of 5.2×10^4 MWd/T and thus are not presented. In comparison to graphite, for the thinnest displacer shells considered (0.01 cm) the typical CANDU discharge burnup is now recovered with an enrichment of 1.6 wt% compared to 1.8 wt% for the graphite displacers. Similarly, for the thickest displacer shells considered (0.05 cm) the results suggest that the enrichment

required to recover the typical CANDU burnup would be less than 1.5 wt% compared to 1.6 wt% for the graphite displacers.

Irrespective of the comparison of values between beryllium and graphite, all the trends noted to this point are preserved i.e.: CVR increases with increasing displacer shell thickness and discharge burnup increases with increasing displacer shell thickness. This supports the assertion that these trends are due to the re-introduction of moderation into the lattice in the form of the displacer material.

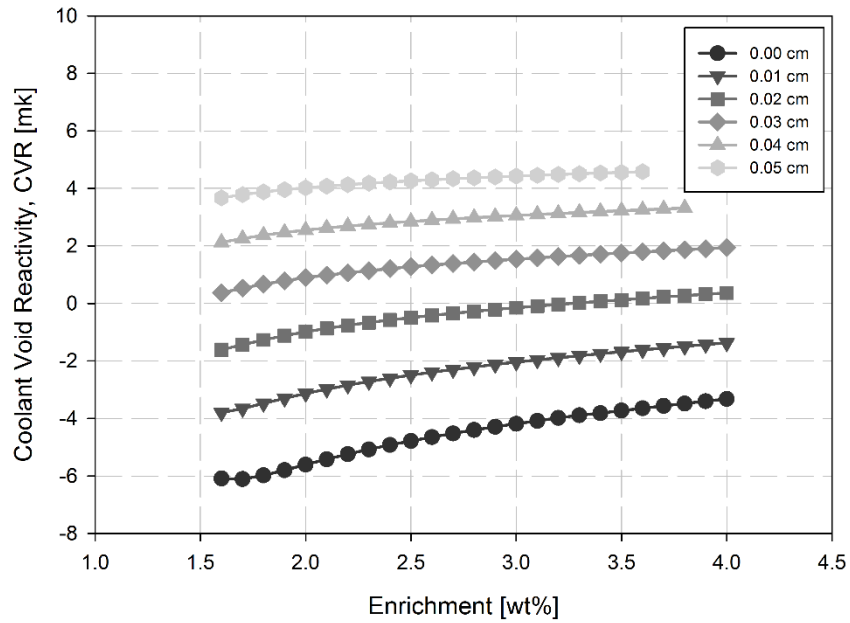


Figure 29 Burnup averaged coolant void reactivity for beryllium displacers.

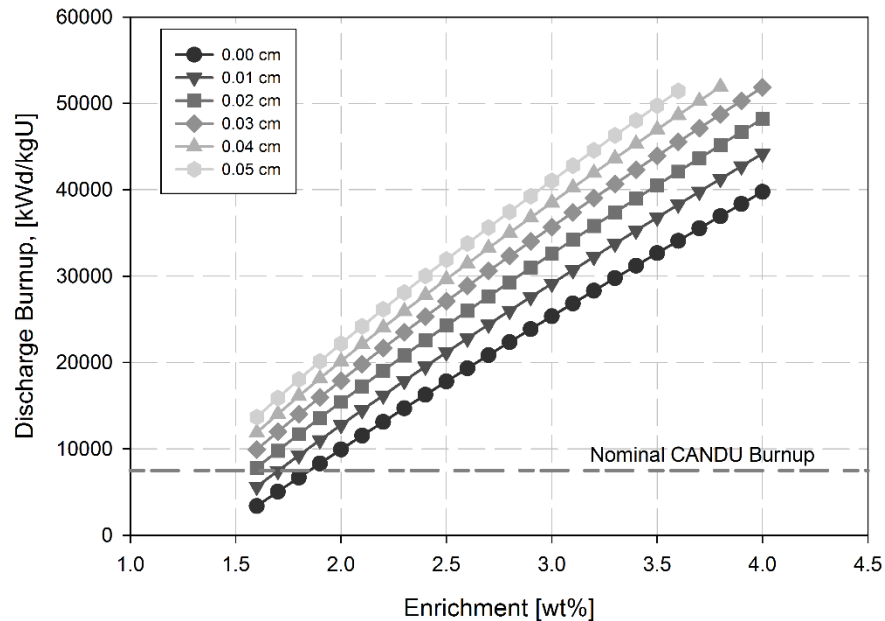


Figure 30 Discharge burnup for beryllium displacers.

Lead:

The next displacer shell material considered is lead. Lead is primarily known as a shielding material though one that does not interact strongly with neutrons making it, from a neutronic if not mechanical perspective, a plausible shell material.

The results for the burnup averaged CVR and discharge burnup as a function of thickness and enrichment are summarized in **Figure 31** and **Figure 32** respectively. Because lead is not a moderator it is not a surprising that the results differ from those of graphite and beryllium. Upon first inspections the results are not dissimilar from those with the zirconium displacers. Similar to zirconium, all burnup averaged CVR values are negative over the range considered. When compared to zirconium a lower enrichment is

required to recover the traditional CANDU burnup; for the thickest displacers considered approximately 2.2 wt% compared with approximately 2.7 wt% for zirconium.

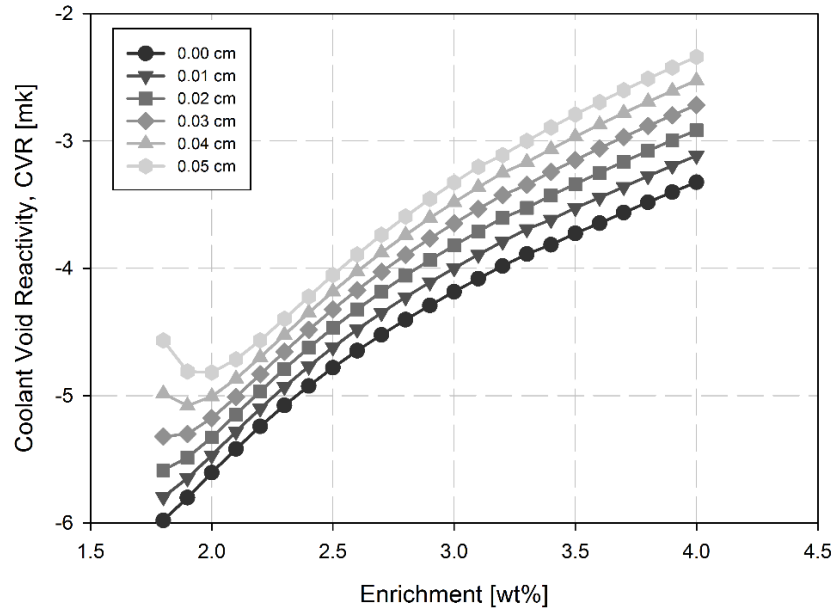


Figure 31 Burnup averaged coolant void reactivity for lead displacers.

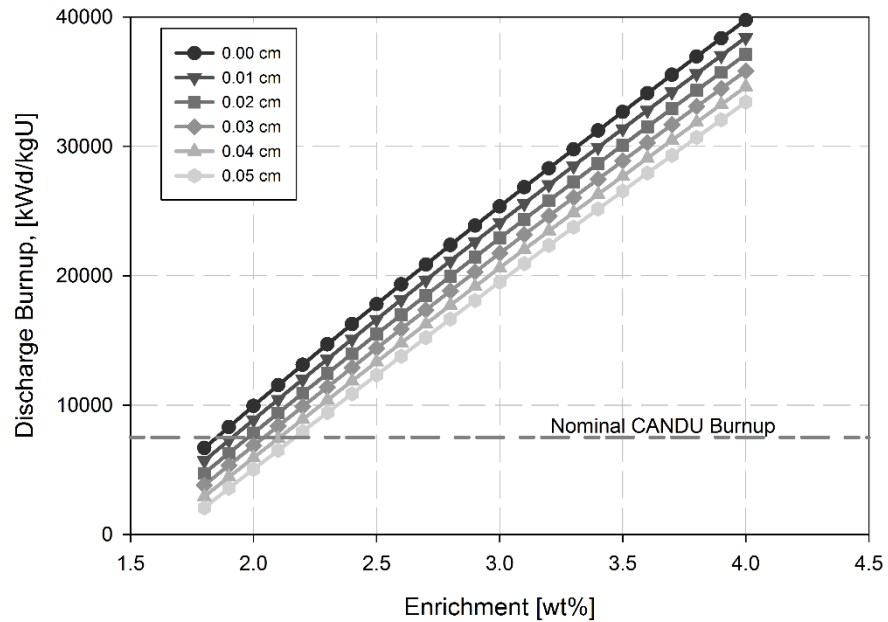


Figure 32 Discharge burnup for lead displacers.

The most distinct difference between zirconium and lead is the opposing trends in burnup averaged CVR with displacer shell thickness. In the case of lead displacers the CVR increases with increasing displacer thickness, however, in the case of zirconium CVR decreases with increasing displacer shell thickness.

The explanation for the difference stems from the change in moderator spectrum upon voiding and from the difference in the energy dependence of the absorption cross sections between lead and zirconium. When the displaced-moderator lattice is voided, the moderator spectrum hardens. This can be seen in both **Figure 33** and **Figure 34** by the difference in moderator flux per unit lethargy between the voided and cooled lattice for the case of 4.0 wt% enrichment. For thin displacers, the moderator spectrum is a good approximation for the spectrum inside the displacer walls. The microscopic absorption cross-sections for the two materials, lead and zirconium, demonstrates a marked difference in their energy dependence. The energy dependence of the microscopic absorption cross-sections for lead and zirconium is presented in **Figure 33** and **Figure 34** respectively for the first burnup step. The absorption cross-section for zirconium exhibits two peaks at energies between 100 eV and 50 keV, while the absorption cross-section for lead trends steadily lower, with few exceptions, for higher energies. As a result of the energy dependence of the absorption cross sections, the total absorption rate increases on voiding for zirconium leading to a lower CVR, whereas it decreases for lead, leading to a higher CVR. The effects are larger for thicker spheres, leading to the observed decrease in CVR with increased thickness for zirconium and increase in CVR with increased

thickness for lead. In short, the zirconium displacers absorb neutrons preferentially in the voided state while the lead displacers do not.

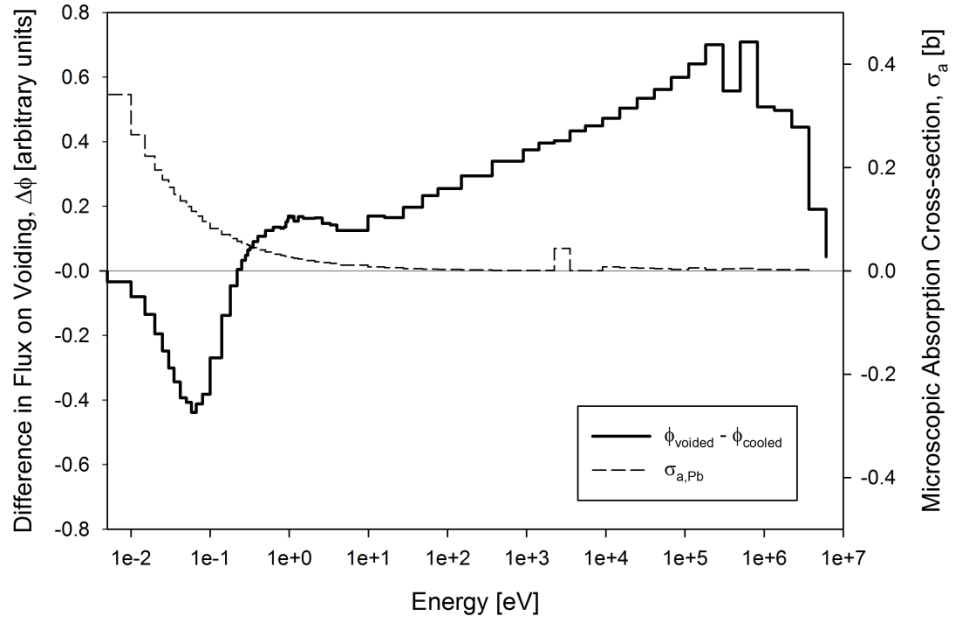


Figure 33 Energy dependence of the microscopic absorption cross-section for lead.

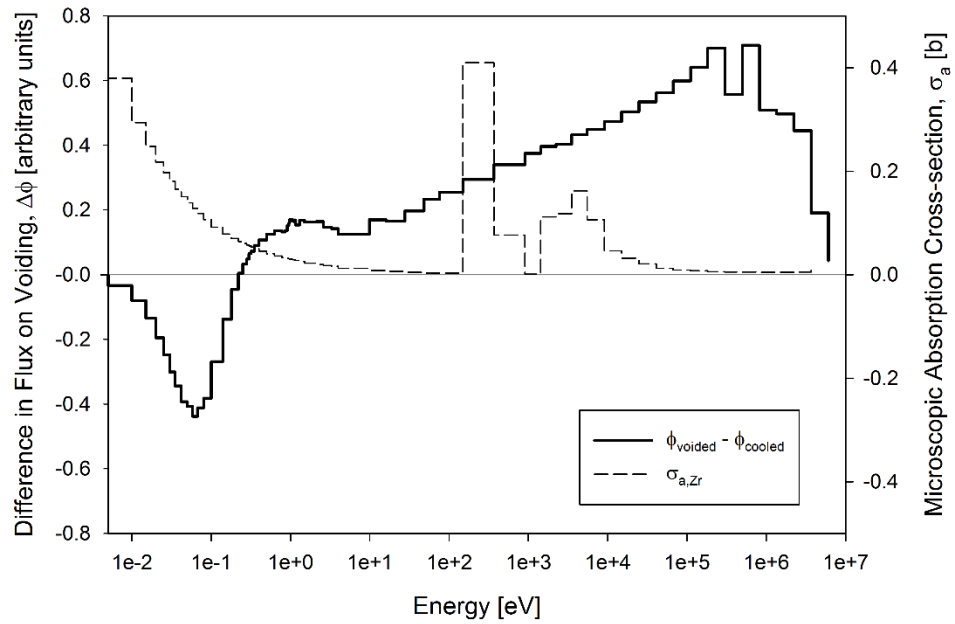


Figure 34 Energy dependence of the microscopic absorption cross-section for zirconium.

The difference in the total absorption reaction rate (all groups), voided minus cooled, visualized as a function of position further illustrates a salient difference in neutronic properties between the two materials. In the case of voiding the fresh lattice with uniformly enriched 2.0 wt% fuel and 0.05 cm thick zirconium displacers it is evident from the difference map, **Figure 35**, that absorption rate in the displacer regions increases upon voiding. In the figure the inner portion of the displacers can be used as a reference. In the cooled case there is practically no absorption as there is effectively no material present absorb neutrons. Similarly, in the voided case again there is practically no absorption for the identical reason. The absolute difference between the two effectively zero absorption rates is effectively zero. However, in the shell material encapsulating the void the difference in absorption rate is clearly higher and thus positive meaning an increase in the absorption rate on voiding.

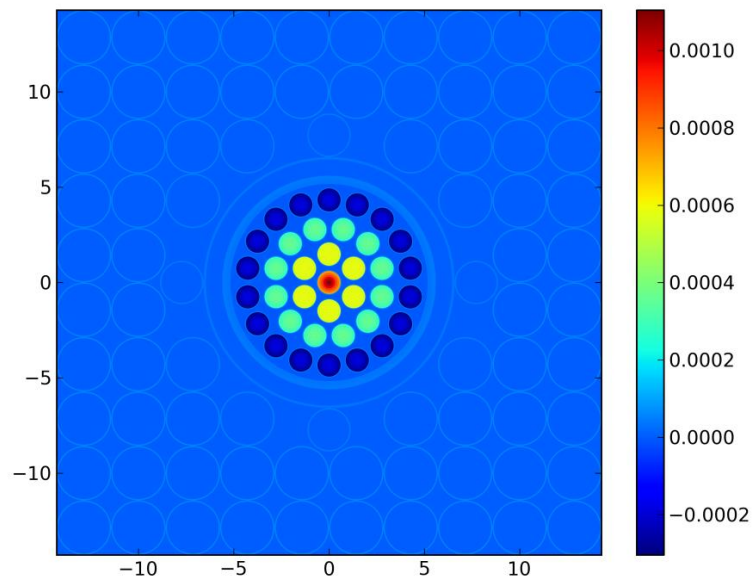


Figure 35 Difference in absorption rate, voided less cooled, as a function of position in the 2.0 wt% enriched lattice with 0.05 cm zirconium displacers.

Conversely, in the equivalent lead displacer case, namely a fresh lattice with uniformly enriched 2.0 wt% fuel and 0.05 cm thick lead displacers, it is apparent that there is a reduction in the absorption in the displacer material on voiding, **Figure 36**.

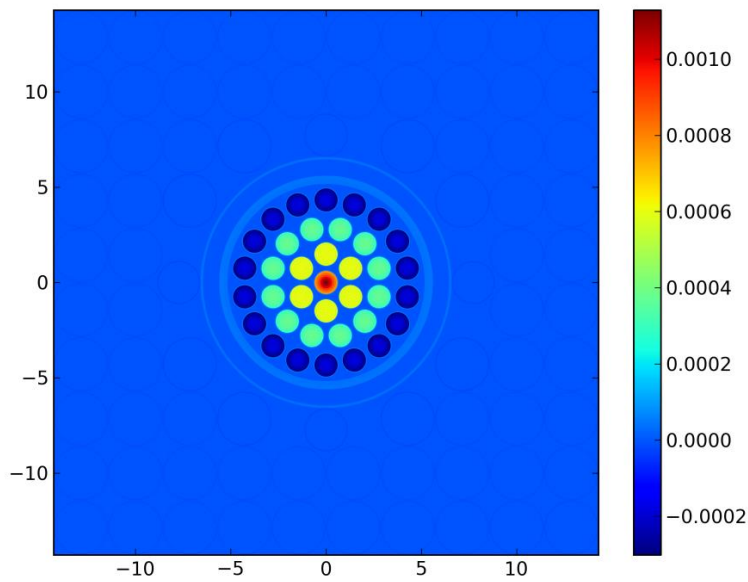


Figure 36 Difference in absorption rate, voided less cooled, as a function of position in the 2.0 wt% enriched lattice with 0.05 cm lead displacers.

Aluminum:

The final displacer material considered is aluminum. Aluminum was among the first materials used to protect reactor in-core components from corrosion induced by coolant (Anderson, 1962). Aluminum is considered here as a potential displacer material.

The burnup averaged CVR and discharge burnup results for aluminum are summarized in **Figure 37** and **Figure 38** respectively. The results are similar to those observed for lead displacers. Much like the one for lead displacers, the CVR for aluminum displacers, **Figure 37**, increases with displacer thickness, with the increase being slightly larger than in the case of lead. For the case of the greatest thickness

simulated, 0.05 cm, and the highest enrichment simulated, 4.0 wt%, the CVR reaches a value of around -1.0 mk, higher than the -2.2 mk observed for lead, but still negative.

The aluminum displacers result in a burnup close to that of zirconium displacers. For the greatest thickness considered, 0.05 cm, a fuel enrichment of approximately 2.7 wt% is required to recover the nominal CANDU burnup. 2.7 wt% is required to recover the nominal CANDU burnup.

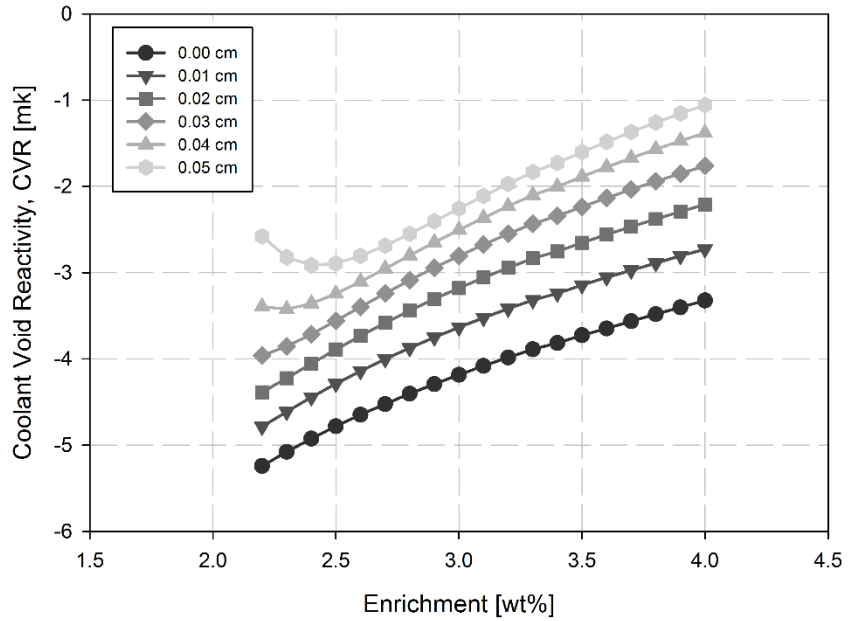


Figure 37 Burnup averaged coolant void reactivity for aluminum displacers.

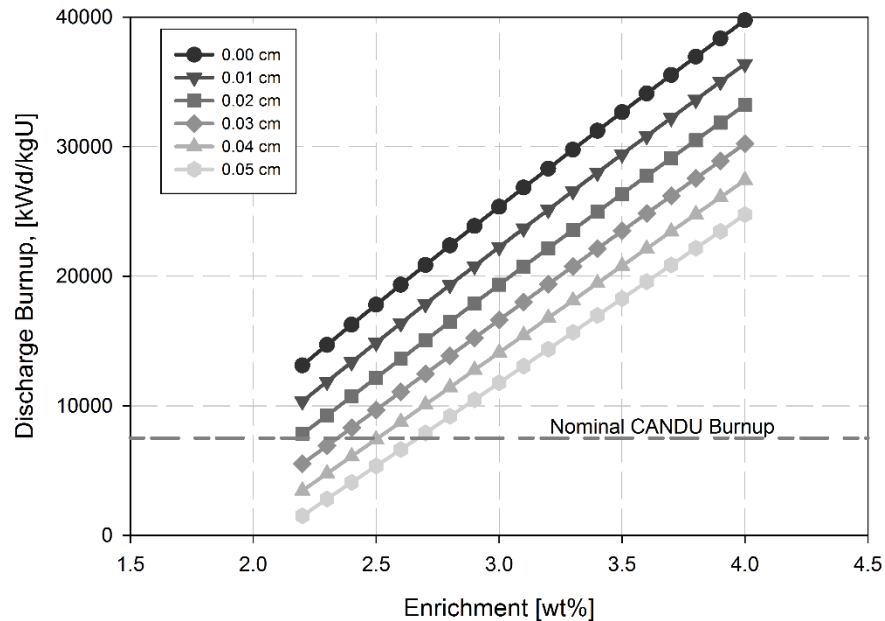


Figure 38 Discharge burnup for aluminum displacers.

Checkerboard Coolant Void Reactivity:

Ultimately the purpose of modifying the CANDU lattice to include displacers is to reduce the reactivity effect on voiding. Until this point a lattice model with reflective boundary conditions has been used to assess this reactivity effect. Simulated voiding of the single-cell infinite lattice is representative of simultaneous uniform voiding of all channels. In a large-break loss of coolant accident, however, the coolant within a CANDU core does not initially void uniformly. Instead, owing to alternating flow directions in adjacent channels the coolant initially voids in alternating channels in a checkerboard pattern.

In traditional CANDU reactors, the reactivity change induced by checker-board voiding is approximately equal to half the reactivity change induced by complete voiding

of the coolant (Popov, 2008). It is a meaningful exercise to ensure this remains the case for a CANDU core retrofitted with displacers. In particular, because the retrofit can render the full-void CVR negative, it is important to determine whether the reactivity change on voiding remains negative in those cases for a checkerboard voiding pattern. Checkerboard voiding is therefore studied for the retrofitted lattice using a 2×2 multi-cell model with periodic boundary conditions. The model is able to accommodate the heterogeneity of differing coolant densities in adjacent channels. In particular, the model is shown in **Figure 39** where two diagonally opposed cells are voided.

The Checker-Board Coolant Void Reactivity (CBCVR) is calculated for each displacer material using 2.0 w% fuel enrichment and a 0.02 cm displacer thickness at three instantaneous burnups. The fuel enrichment and displacer thickness were selected such that for each displacer material the CVR was negative and the projected exit burnup was reasonable. The three instantaneous burnups correspond to near fresh (but with saturating fission products), near the mid-burnup of a traditional CANDU reactor and near the average discharge burnup of a traditional CANDU reactor (although it is important to note that the burnup values do not necessarily correspond to the mid-burnup and discharge burnup for that particular material, thickness and enrichment combination). Additionally, the CBCVR for the ideal zero-thickness displacers is also calculated.

The CBCVR and full-void CVR are summarized for the three burnups in **Table 12** below. The results indicate that, similarly to the situation in traditional CANDU lattices, the CBCVR is approximately half of the full-void CVR. Implicitly, the negative sign of the retrofitted-lattice CVR is preserved on checker-board voiding. It is then reasonable to deduce from the linearity of the results that checker-board modelling

refinement is not essential to evaluation of the coolant voiding induced reactivity change in the retrofitted lattice conducted to this point.

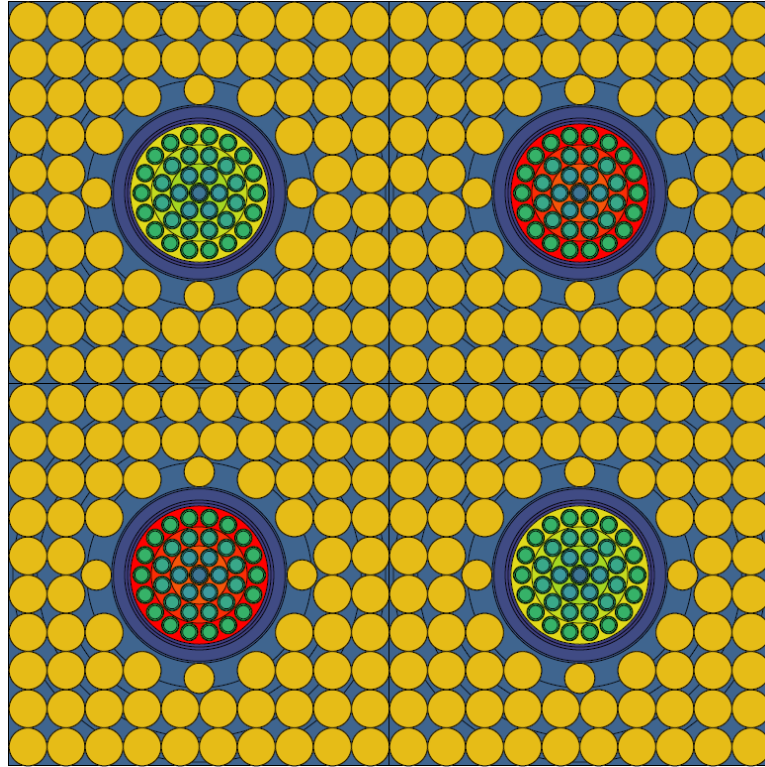


Figure 39 Checker-board pattern voiding of coolant in a 2x2 cell model – diagonal cells are voided.

Table 12 Summary of CBCVR and full-void CVR for Various Materials at a Thickness of 0.02 cm and Fuel Enrichment of 2.0 wt%

	Burnup = 0.2 MWd/kgU		Burnup = 3.6 MWd/kgU		Burnup = 7.6 MWd/kgU	
	CBCVR (mk)	CVR (mk)	CBCVR (mk)	CVR (mk)	CBCVR (mk)	CVR (mk)
zero thickness	-2.181	-5.026	-2.706	-5.996	-2.276	-5.035
Zirconium	-2.410	-5.584	-2.970	-6.624	-2.543	-5.667
Graphite	-1.763	-4.072	-2.210	-4.960	-1.774	-3.993
Beryllium	-1.117	-2.726	-1.530	-3.507	-1.056	-2.505
Lead	-2.118	-4.869	-2.619	-5.858	-2.185	-4.885
Aluminum	-1.900	-4.519	-2.445	-5.525	-2.001	-4.534

Fuel Cycle Costs:

One of the central compromises associated with the introduction of moderator displacers into the CANDU lattice is fuel cycle cost. The loss of moderation within the lattice requires that the fuel be enriched in order to recover CANDU-typical values of fuel utilization. Because the use of displacers requires enriching the fuel, the fuel-cycle cost will be affected. At the front end, the cost of enriched fuel will be higher than the cost of non-enriched fuel. At the back end, to the extent that no increase in the discharge burnup compared to the non-retrofitted case is envisaged, the volume of discharged spent fuel is expected to be similar for the retrofitted and non-retrofitted reactors. However, enriched-uranium spent fuel will contain a larger amount of fissile elements than natural-uranium spent fuel, will have a higher reactivity and therefore, unlike the natural-uranium spent fuel, may require some additional measures to accommodate the more reactive spent fuel. Estimating the cost associated with such facilities would be cumbersome and the calculated value would have a large margin of uncertainty. This section therefore focuses only on a simple analysis of the front-end fuel cost implications of the proposed retrofit i.e. the introduction of moderator displacers. The method of estimating fuel cost is that presented by (Tsoulfanidis, 2013). For this simple analysis, the conversion losses, which are usually in the range of 1%, are neglected. The necessary fuel enrichment is determined by the displacer material, displacer-wall thickness and the desired discharge burnup. For a fair comparison of fuel costs, the discharge-burnup of the retrofitted reactor is kept equal to the discharge burnup of the non-retrofitted reactor.

The mass-unit price of enriched uranium, PE, can be expressed as a function of the natural-uranium price, PU, the conversion price, PC, and the Separative-Work-Unit (SWU) price, PS:

$$PE = (PU + PC) \cdot \left(\frac{x_p - x_w}{x_f - x_w} \right) + PS \cdot SF \quad (5)$$

In Eq. (5), x_p , x_f , x_w are the ^{235}U weight fractions of the enriched uranium, natural uranium (feed material) and depleted uranium respectively, and SF is the SWU factor, defined as the number of SWUs per unit mass enriched uranium produced. The SWU factor can be expressed as¹²:

$$SF = V(x_p) + \left(\frac{x_p - x_f}{x_f - x_w} \right) \cdot V(x_w) - \left(\frac{x_p - x_w}{x_f - x_w} \right) \cdot V(x_f) \quad (6)$$

In the above equation, $V(x)$ is the separation potential calculated as:

$$V(x) = (2x - 1) \cdot \ln \left(\frac{x}{1 - x} \right) \quad (7)$$

The total price of the fuel per unit mass of uranium, PT, is calculated as the sum of the mass-unit price of enriched uranium, PE, and the price of fabrication per uranium mass unit, PF:

$$PT = PE + PF \quad (8)$$

Equations (5) – (8) are used to determine the enriched fuel price, the non-enriched fuel price (by ignoring the terms that apply to enrichment) and, subsequently, their ratio, which defines the relative fuel cost for a retrofitted reactor with respect to an un-

retrofitted one. Estimates of price components corresponding to year 2011 are taken from (Tsoulfanidis, 2013) and shown in **Table 13**.

Table 13 Price Components of Nuclear Fuel (year 2011) (Tsoulfanidis, 2013)

Uranium, PU	\$155/kgU
Conversion, PC	\$10/kgU
Enrichment, PS	\$110/kg-SWU
Fabrication, PF	\$200/kgU

Relative fuel costs for different displacer materials are subsequently calculated for a 0.02 cm displacer-wall thickness. Results are shown in **Table 14** in the row marked “reference”. To investigate the influence that variations in major price components have on the overall relative fuel cost, each major price component is varied, first by being halved and then by being doubled. Relative fuel costs corresponding to varied price components are also included in **Table 14**.

The “reference” values in **Table 14** show a 2.3- to 3.2-fold increase in the fuel cost, depending on the chosen displacer material, at the reference values of the price components. Not surprisingly, the displacer materials that also serve as a moderator, namely beryllium and graphite, correspond to the lowest enrichments and therefore lowest relative cost increases; factors of 2.3 and 2.5 respectively. Of the non-moderating displacer materials lead has the next lowest relative cost increase at 2.9 followed by zirconium and aluminum with nearly identical relative cost increases of 3.2.

In terms of the sensitivity of the relative cost to variations in the cost components **Table 14** shows that the relative fuel cost displays only modest sensitivity (approx. 15%) to a halving or doubling of the price of uranium, PU, historically the most volatile of the price components. The relative fuel cycle cost is sensitive to the price of fabrication, PF, as this is a dominant price component of the unenriched fuel. Reducing the cost of fabrication significantly reduces the cost of the unenriched fuel but influences the price of the enriched fuel substantially less. Consequently, halving the price of fabrication can increase the relative fuel cost to as much as 4.1 for the materials with the highest enrichment.

Table 14 Relative Fuel Cost for Different Displacer Materials (0.02 cm displacer wall-thickness)

varied cost component	Displacer Material (²³⁵ U enrichment - wt%)				
	Zirconium (2.2 wt%)	Graphite (1.7 wt%)	Beryllium (1.6 wt%)	Lead (2.0 wt%)	Aluminum (2.2 wt%)
reference	3.2	2.5	2.3	2.9	3.2
PU=0.5×PU _{ref}	2.9	2.2	2.1	2.6	2.9
PU=2.0×PU _{ref}	3.7	2.7	2.6	3.3	3.7
PF=0.5×PF _{ref}	4.1	3.0	2.8	3.7	4.1
PF=2.0×PF _{ref}	2.5	1.9	1.8	2.2	2.5
PS=0.5×PS _{ref}	2.9	2.3	2.1	2.7	2.9
PS=2.0×PS _{ref}	3.9	2.8	2.6	3.4	3.9

Introducing moderator displacers necessitates the enrichment of fuel which increases the cost of the retrofitted core relative to the nominal one. Potentially offsetting at least a portion of this increased cost is the value of the heavy water moderator that is

displaced and no longer needed. Assuming a heavy water price of \$300/kg (Miller, A, 2001) the total value of the displaced heavy water in a typical CANDU-6 reactor can be estimated to be similar to the increase in yearly fuelling cost associated with the assumption in *Table 14*.

Graded Enrichment:

To reclaim the fuel utilization lost to the displaced moderator the fuel was enriched. In the scoping studies presented to this point the enrichment distribution was assumed to be uniform. However, as discussed in Chapter 2, the grading of enrichment within a bundle has been shown to have a favourable influence on reducing the coolant void reactivity. Because changes to the fuel are mandated by the retrofit it is only an incremental effort to include additional changes to the fuel design like enrichment grading. In this way, the manipulation of the coolant void reactivity gains an additional degree of freedom without introducing much more complexity as the fuel is already being changed.

A cursory exploration, to probe the potential benefit of graded enrichment in terms of CVR, can be carried out using two fuel enrichments in the retrofitted lattice with vanishingly small displacers (the no material case). For the sake of simplicity, the lower enrichment is always considered to be natural uranium applied to either the centre pin only or the central 7 elements of the fuel; not dissimilar to the design proposed in (Dastur, et al, 1992) and presented in *Figure 14b*. Natural uranium is considered to be suitable as it is already used as the primary fuel in conventional CANDU reactors; indeed using natural enrichment in some fuel elements can be envisaged as simply forgoing the

enrichment of those elements. The results for both graded enrichment schemes are presented in *Figure 40* and *Figure 41* for CVR and discharge burnup respectively.

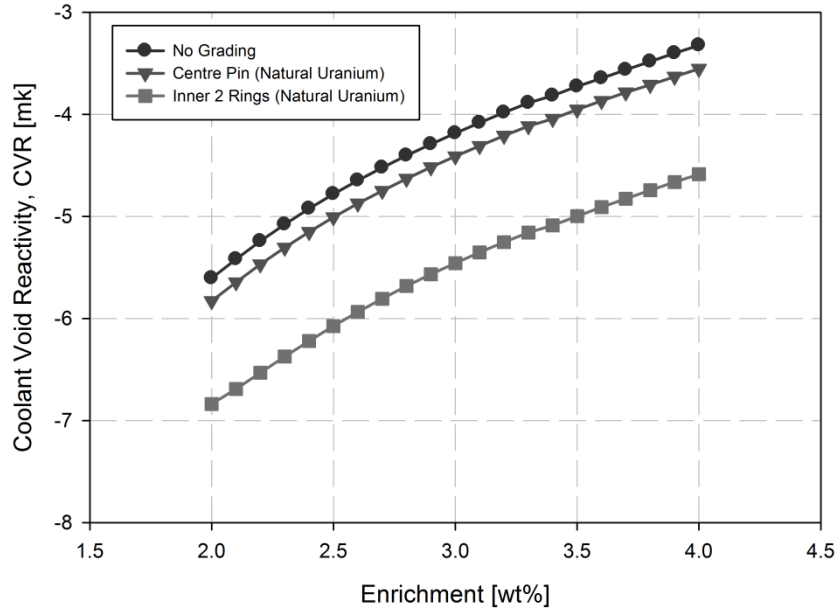


Figure 40 Coolant void reactivity in a displaced lattice cell with graded enrichment.

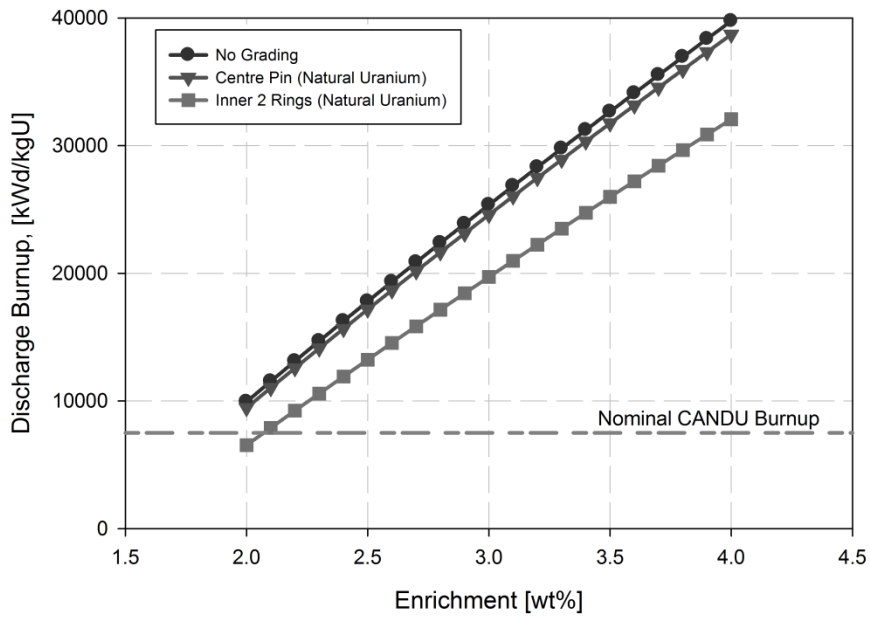


Figure 41 Discharge burnup in a displaced lattice cell with graded enrichment.

What can be seen in *Figure 40* and *Figure 41* is that the graded enrichment with the natural uranium distributed in the centre of the bundle serves to augment the reduction in coolant void reactivity. However, the enhancement in CVR performance gained from grading the enrichment comes at the expense of discharge burnup. This levy on fuel utilization is like the decrease in burnup observed when the moderator displacers are introduced. Both changes serve to decrease CVR and discharge burnup. A conceivable implementation may use both approaches in concert. For instance, the displacers can achieve a maximum displacement ratio of ~74%. Presumably, if perforated displacers that allow moderator permeate them (i.e. are not filled with void) are used judiciously displacement ratio can be engineered to be essentially any value less than ~74%. On the other hand, the degree of enrichment in the outer rings effectively determines the degree to which graded enrichment is used to influence the coolant void reactivity – the higher the enrichment the more absorbing the centre pins are in a relative sense. To get an idea of the ideal compromise between the two methods of reducing CVR depends on the relative importance between CVR and fuel utilization among other things.

A rudimentary comparison of the benefits can be done by comparing the CVR reduction gained from, and burnup lost to, the introduction of graded enrichment to the results associated with moderator density changes akin to those engineered by the addition of moderator displacers. Specifically, using 2.0 wt% as an example, the simulation results used to produce *Figure 21* can be used as a point of comparison. From those results the cost of reducing CVR in terms of discharge burnup is 1.24 mk/MWd/kgU about the maximum displaced case, whereas as for each of the grading options, centre pin and the inner two rings, it is 0.47 mk/MWd/kgU and

0.36 mk/MWd/kgU respectively. Moreover, it is worth mentioning that the effects of enrichment grading offer diminishing returns with increased absorption. For example if depleted uranium (with a hypothetical enrichment of 0.5 wt%) is used as the centre pin material in the otherwise 2.0 wt% the results in terms of CVR and discharge burnup remain similar as does the cost of reducing CVR with a value of 0.47 mk/MWd/kgU (identical to the significance provided). Similarly, the addition of zirconium also reduces the CVR only with a reduction cost of 0.23 mk/MWd/kgU. These results suggest that in the lattice with displacers with a 2.0 wt% enriched fuel the displacement of moderator remains inexpensive in terms of burnup compared to enrichment grading. A comparison of the CVR reduction costs are summarized in **Table 15**. It should be noted that the values presented in **Table 15** only apply to the displaced lattice. For example in the nominal lattice the displacement of small amounts of moderator is not an effective means of reducing the CVR as suggested by **Figure 21**.

Table 15 Comparison of the Cost in Terms of Discharge Burnup of Different Means of Reducing CVR in a CANDU Lattice with Close-packed Displacers

Method of Reducing CVR	CVR Reduction Efficiency (mk/MWd/kgU)
Centre Pin Natural Uranium	0.47
Centre Pin Depleted Uranium (0.5 wt%)	0.47
Central 2 rings Natural Uranium	0.36
Displacing moderator	1.24
Adding Zirconium in moderator	0.23

These rudimentary results do not consider increased cost of fuel fabrication for a more complex bundle nor the reduced fuel material cost associated with the reduction of enriched fuel in the bundle. Nor does the comparison assess important performance or safety aspects like the linear element rating. They are just provided as a cursory comparison of alternate (or complementary) means to reduce the coolant void reactivity.

Chapter VI Conclusions

The primary conclusion that can be drawn from the presented work is that the displacement of moderator using naturally-arranged close-packed spherical displacers reduces the CVR of a CANDU lattice to varying degrees depending on material, thickness and enrichment. Negative CVR is achieved for certain materials and displacer-wall thicknesses. Checkerboard voiding does not present any special concerns as CBCVR values are approximately half of those for full-void CVR and the negative sign of the full-void CVR is preserved in the case of checkerboard voiding.

The mechanism exploited to reduce the coolant void reactivity is the reduction of the moderator-to-fuel ratio such that the voiding of coolant increasingly constitutes a loss of moderation. Specifically, the displacement achieved through the use of hexagonally packed spherical displacers is often sufficient to invert the sign of the reactivity effect in the CANDU lattice.

To accommodate changes in fuel utilization due to the diminished moderation and increased absorption in the lattice cell, the fuel must be enriched. Enriching the fuel presents the opportunity to adjust the discharge burnup. If the discharge burnup is kept unchanged, the need for enrichment leads to between a 2.5- and a 3.2-fold increase in fuel costs for the retrofitted reactor compared to the non-retrofitted one, depending on displacer thickness and material.

From a neutronic perspective, all studied materials, with the exception of stainless steel, are acceptable for manufacturing the displacers within certain ranges of thickness. The final choice of material will therefore have to rely on other considerations. A cursory

review shows that beryllium is the most attractive displacer material from a fuel cost perspective, but its high cost and toxicity may make it undesirable. Graphite is next best after beryllium in terms of front-end fuel cost, however it may be less desirable for mechanical considerations, specifically brittleness. Similarly, lead may be unattractive because of its softness. This leaves aluminum and zirconium as the most attractive choices. Aluminum is preferable from a material cost perspective while zirconium has the advantage of substantial CANDU in-reactor experience.

While it is the intent of this work to provide useful scoping studies pertaining to close-packed spherical moderator displacers the work primarily focusses on the reactor physics implications. Several important considerations that fall outside of the field of physics are not addressed. For instance, reducing the amount of water in the form of moderator surrounding the core may be disadvantageous in some accident scenarios. Or, the impact of filling the calandria with small spherical displacers on the moderator temperature distribution and management during normal operation is not considered, nor is the potentially adverse impact on moderator circulation or the moderator poison shutdown system. Aging of the displacers themselves is not considered and neither is the consequence of their failure. Even certain parameters associated with reactor physics are not considered, for instance an evaluation of the effect of enrichment and displacers on the linear element rating within the fuel. The preceding are a few examples, by no means an exhaustive accounting, of some of the issues that would have to be considered prior to implementation of the retrofitted lattice.

Chapter VII Future Work

The work described above introduces the possibility for future work expanding on what has been done to date. From a modelling perspective, future investigations should include confirmatory work using a three-dimensional model and an alternate transport code, such as MCNP. Future full-core calculations will have the ability to remove the need for some of the assumptions associated with lattice level modelling – particularly in terms of distributed properties and in the estimation of average discharge burnup. Use of an alternate transport code would provide a point comparison and reinforce many of the results and observations made in the work above.

Additionally, although challenging to implement, the use of multiple materials for the displacers may prove worth exploring. The results above have shown that different materials can give rise to disparate results in terms of the CVR and fuel economy. It may be possible to introduce a method to tune these results by using multiple displacer types. Varying displacer types can be introduced by having layered displacers, **Figure 42**, or by having more than one displacer type distributed throughout the core, **Figure 43**. It is even conceivable that spatial dependence of displacer material within the core may impart some advantage. Even if judged to be infeasible or impractical the study of multiple-material displacers is worthwhile in an academic context.

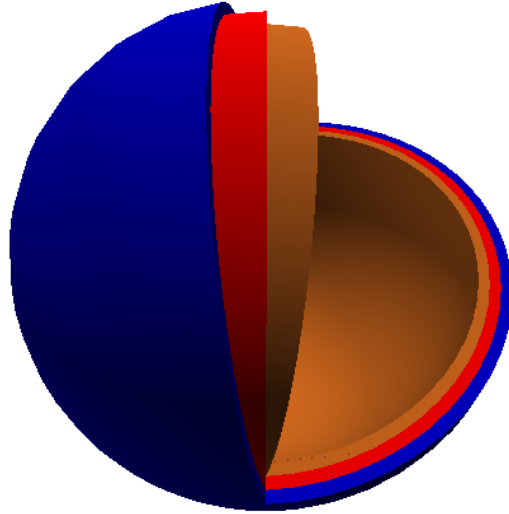


Figure 42 A layered displacer where each color represents a different material.

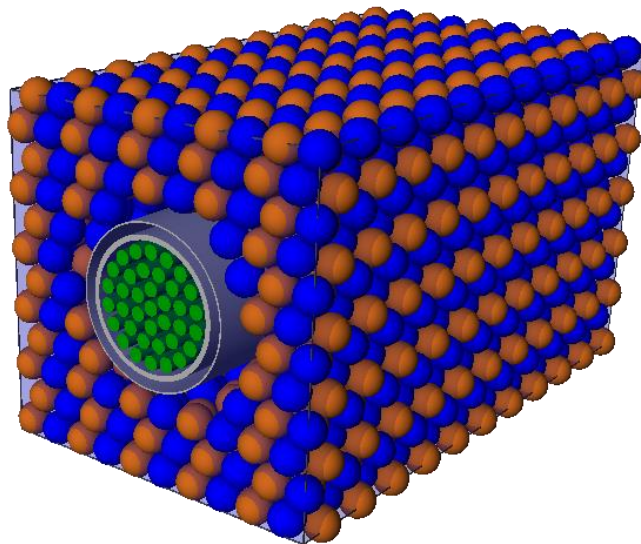


Figure 43 A distribution of displacers where each color represents a different material.

To reclaim the fuel utilization lost to the displaced moderator the fuel was enriched. For the purposes of the work presented the enrichment was assumed to be

uniform. However, as discussed previously in Chapter II the grading of enrichment within a bundle has been shown to have a favourable influence on reducing the coolant void reactivity. Because changes to the fuel are mandated by the retrofit, it may be beneficial to include further fuel design considerations while the bundle composition is being revisited, expanding on the cases presented in Chapter IV, in further study of moderator displacers. This way the reduction of coolant void reactivity gains an additional degree of freedom without introducing much more complexity as the fuel is already being changed.

Finally, the introduction of moderator displacers changed the reactivity effect of voiding the coolant. For the un-retrofitted CANDU lattice (Whitlock, 1995) has categorized and quantified the components of the CVR. No such quantification was performed in this work, however, in future it would be valuable to perform an equivalent analysis, repeating the original effort with the un-retrofitted lattice and comparing the new components that produce the coolant void reactivity in the retrofitted lattice.

References

- Anderson W, Beck, C., Kephart, A., Theilacker, J., "Reactor Structural Materials: Engineering Properties as Affected by Nuclear Reactor Service", ASTM Special Technical Publication No. 314, 1962.
- ANL-5800, "Reactor Physics Constants", Argonne National Labs, Second Edition, 1963.
- Baker, D. E., "Graphite as a Neutron Moderator and Reflector Material", Nuclear Engineering and Design 14, 1970.
- Beeston, J.M., "Beryllium Metal as a Neutron Moderator and Reflector Material", Nuclear Engineering and Design 14, 1970.
- Boczar, P. G., Blundell, H. G., Dyck, M. T. "Fuel Management Simulations for a Part-core Loading of Slightly Enriched Uranium in a CANDU-600", 8th Annual CNS Conference, 1987.
- Boczar, P. G., et al, "A Low-void Reactivity CANDU Fuel Bundle", Proc. 3rd International Conference on CANDU Fuel, 1992.
- Boczar, P. G., Sullivan, J. D., "Low Void Reactivity Fuel", 25th Annual CNS Conference, 2004.
- Bonalumi, R. A., Lau, J.H.K., "Technical Aspects and Economic Promise of Low-Enriched Uranium CANDU-PHW Reactors", 1st Annual CNS Conference, 1980.
- Buijs, A., et al, "The Physics Design of the Advanced CANDU Reactor", International Conference on the Physics of Reactors, 2008.
- Carlson, R. L., Sendelbeck, R. L., Hoff, N. J., "Experimental Studies of the Buckling of Complete Spherical Shells", Experimental Mechanics, 7, 1967.
- Chan, P. S. W., Dastur, A. R., "The Role of Enriched Fuel in CANDU Power Upgrading", 8th Annual CNS Conference, 1987.
- Chan, P. S. W., et al, "CANDU – a Versatile Reactor for Plutonium Disposition or Actinide Burning", Proc. International Conference on Future Nuclear Systems, 1997.
- Cotton, C., et al, "Coolant Void Reactivity Analysis of CANDU and ACR-700 Lattices", Transactions of the American Nuclear Society, 90 587, 2004.
- Cotton, C., et al, "Physics Analysis of Coolant Voiding in the ACR-700", Transactions of the American Nuclear Society, 92 685, 2005.
- Dastur, A. R., Buss, D. B., "The Influence of Lattice Structure and Composition on the Coolant Void Reactivity in CANDU", 11th Annual CNS Conference, 1990.
- Dastur, A. R., Chan, P. S. W., Bowslaugh, D., "The use of Depleted Uranium for the Reduction of Void Reactivity in CANDU Reactors", 13th Annual CNS Conference, 1992.
- Duderstadt, J., Hamilton, L., "Nuclear Reactor Analysis", John Wiley and Sons, 1976.

- Farkas, R. and Nichita, E., "Preliminary Comparison of Transport Codes Applied to a Second-Generation PT-SCWR Lattice", 2014 Canada-China Conference on Advanced Reactor Development, Niagra Falls, Ontario, 2014.
- Green, R. E., "Reactivity Effects of Moderator Voids in a CANDU Lattice", AECL Technical Report (publically available) AECL-3002, 1968.
- Hicks, D., Johnstone, I., O'Dell, F. P., "Nuclear Design of SGHWRs", Steam Generating and Other Heavy Water Reactors, 1968. *⁵
- Khatchikian, F., Fink, J., "Void Reactivity Studies for the Atucha-II PHWR Reactor. Preliminary Design of a Lower Void Reactivity Fuel", 29th Annual CNS Conference, 2008.
- Kim, S. Y., Suk, H. C., "A study on Performance of Adjuster Rod System and Banking Scheme in Operational Transient of CANDU-6 RUFIC Core", Proceedings of the Korean Nuclear Society Autumn Meeting, 2002.
- Lang, L., "Beryllium: A Chronic Problem", Environmental Health Perspective 102(6-7), 1994.
- Leszczynski, F., López Aldama, D., Trkov, A., "WIMS-D library update: final report of a coordinated research project", Vienna, International Atomic Energy Agency, 2007.
- MacGillivray, G. M., Hastings, I. J., "Slightly Enriched Uranium Fuel Cycle: Performance Aspects", 7th Annual CNS Conference, 1986.
- Marleau, G., Herbert, A., Roy, R., "A User Guide for DRAGON 3.05E", Ecole Polytechnique de Montreal, 2007.
- Miller, A., "Heavy Water: A Manufacturers' Guide for the Hydrogen Century", Canadian Nuclear Society Bulletin 22, 2001.
- Min, B. J., Kim, B. G., Sim, K-S., Suk, H.C., "The Use of Graphite for the Reduction of Void Reactivity in CANDU Reactors", 4th International Conference on CANDU fuel, 1995.
- Nichita, E. "Retrofitting CANDU Reactors for Negative Coolant Void Reactivity", Trans. Am. Nucl. Soc. 99, 717, 2008.
- Popov, A., et al, "Models for coolant void reactivity evaluation in CANDU Generation II and III+ Reactors", International Conference on the Physics of Reactors, Interlaken, Switzerland, 2008.
- Ovanes, M., Chan P. S. W., "Reactor Physics Innovations in the ACR-700 Design for the Next CANDU Generation", 23th Annual CNS Conference, 2002.
- Pencer, J., and Colton, A., "Progression of the Lattice Physics Concept for the Canadian Supercritical Water Reactor", Proceedings of the 34th Annual Conference of the Canadian Nuclear Society, Toronto, Ontario, 2013 June 9-12.

⁵ Additional discussion pertaining to this paper appears in the 'Session B: Discussion' portion of the conference proceedings.

- Pickman, D., Gittus, J., Rose, K., "Fuel for the SGHWR", Advances in Nuclear Science and Technology, 1979.
- Rippon, S., "Not Such a Bad Reactor", New Scientist, 1974.
- Roshd, M. H. M., French, P. M., Jones, R. T. , "Nuclear Fuel Bundle Design with Reduced Void Effect", Transactions of the American Nuclear Society, 26 603, 1977.
- Rozon, D., Tajmouati, J., "Simplified Models for the Calculation of The Time-Average Power Distribution in CANDU Reactors Including The Influence of Local Parameters", Proceedings of the 12th CNS Annual Conference, June 4-7, 1991, Saskatoon, SK, 1991.
- Tsoufanidis, N., "The Nuclear Fuel Cycle", American Nuclear Society, 2013.
- Ward, A. et al, "The Application of the PARCS Neutronics Code to the Atucha-I and Atucha-II NPPS", International Conference on the Physics of Reactors, 2008.
- Whitlock, J. J., "Reduction of the Coolant Void Reactivity Effect in a CANDU Lattice Cell", Open Access Dissertations and Theses, Paper 3508, 1995.
- Whitlock, J. J., Garland, W. J., Milgram, M. S., "Effects Contributing to Positive Coolant Void Reactivity in CANDU", ANS Annual Meeting, June 1995.
- Wray, D., Butterfield, M., McMillan, R. "Control of SGHWRs" , Steam Generating and Other Heavy Water Reactors, 1968.

Appendix A Example DRAGON Input File

An example of a DRAGON input is provided below. For clarity it does not correspond to the inputs used in the production of the work described above. Instead it is taken directly from the examples provided with the DRAGON user's manual or from the DRAGON website (http://www.polymtl.ca/nucleaire/DRAGON/en/documentation/S4IGE174R5.php#tth_sEc4.4.7, retrieved August 16, 2014).

```
*-----
* TEST CASE TCWD07
* CANDU-6 CARTESIAN CELL
* WIMSD4 69 GROUPS LIBRARY FILE WNEALIB
* TEST VARIOUS LEAKAGE OPTIONS
*
* REF: R. Roy et al. Ann. Nucl. Energy 21, 115 (1994)
*
*-----
* Define STRUCTURES and MODULES used
*-----
LINKED_LIST
  LIBRARY CANDU6S CANDU6T CANDU6SV CANDU6TV TRACK
  SYS FLUX EDITION ;
MODULE
  GEO: EXCELT: LIB: SHI: ASM: FLU: EDI:
  DELETE: END: ;
SEQ_BINARY
  INTLIN ;
*-----
* Microscopic cross sections from file WNEALIB format WIMSD4
*-----
LIBRARY := LIB: ::
  EDIT 0 NMIX 10 CTRA WIMS
  MIXS LIB: WIMSD4 FIL: WNEALIB
  MIX 1 560.66 0.81212 O16 = '16' 7.99449E-1
    D2D2O = '8002' 1.99768E-1 H1H2O = '2001' 7.83774E-4
  MIX 2 560.66 6.57
    BNat = '11' 2.10000E-4
    Zr91 = '91' 9.75000E+1
  MIX 3 345.66 0.0014 He4 = '4' 1.00000E+2
  MIX 4 345.66 6.44 Fe56 = '56' 1.60000E-1
    Ni58 = '58' 6.00000E-2 Cr52 = '52' 1.10000E-1
    BNat = '11' 3.10000E-4
    Zr91 = '91' 9.97100E+1
  MIX 5 345.66 1.082885 O16 = '16' 7.98895E-1
    D2D2O = '8002' 2.01016E-1 H1H2O = '2001' 8.96000E-5
  MIX 6 941.29 10.4375010 O16 = '16' 1.18473E+1
    U235 = '235' 6.27118E-1 1 SHIB '235.4'
    U238 = '238' 8.75256E+1 1 SHIB '238.4'
  MIX 7 COMB 6 1.0
  MIX 8 COMB 6 1.0
  MIX 9 COMB 6 1.0
  MIX 10 560.66 6.44 Fe56 = '56' 1.60000E-1
    Ni58 = '58' 6.00000E-2 Cr52 = '52' 1.10000E-1
    BNat = '11' 3.10000E-4
    Zr91 = '91' 9.97100E+1
  ;
*-----
```

```

* Geometry CANDU6S : GEOMETRY FOR SELF-SHIELDING (NO VOID)
* CANDU6F : GEOMETRY FOR TRANSPORT (NO VOID)
* CANDU6FV: GEOMETRY FOR TRANSPORT (COOLANT VOID)
* CANDU6FV: GEOMETRY FOR TRANSPORT (COOLANT VOID)
*-----
CANDU6S := GEO: :: CARCEL 5
X+ REFL X- REFL MESHX -14.2875 14.2875
Y+ REFL Y- REFL MESHY -14.2875 14.2875
RADIUS 0.00000 5.16890 5.60320 6.44780 6.58750 14.00
MIX 1 2 3 4 5 5
CLUSTER ROD1 ROD2 ROD3 ROD4
::: ROD1 := GEO: TUBE 2 MIX 6 10 NPIN 1 RPIN 0.0000 APIN 0.0000
RADIUS 0.00000 0.6122 0.6540 ;
::: ROD2 := GEO: ROD1 MIX 7 10 NPIN 6 RPIN 1.4885 APIN 0.0000 ;
::: ROD3 := GEO: ROD1 MIX 8 10 NPIN 12 RPIN 2.8755 APIN 0.261799 ;
::: ROD4 := GEO: ROD1 MIX 9 10 NPIN 18 RPIN 4.3305 APIN 0.0 ;
;
CANDU6T := GEO: CANDU6S :: SPLITR 6 1 1 1 10
::: ROD1 := GEO: ROD1 SPLITR 2 1 ;
::: ROD2 := GEO: ROD2 SPLITR 2 1 ;
::: ROD3 := GEO: ROD3 SPLITR 2 1 ;
::: ROD4 := GEO: ROD4 SPLITR 2 1 ;
;
CANDU6SV := GEO: CANDU6S :: MIX 0 2 3 4 5 5 ;
CANDU6TV := GEO: CANDU6SV :: SPLITR 6 1 1 1 10
::: ROD1 := GEO: ROD1 SPLITR 2 1 ;
::: ROD2 := GEO: ROD2 SPLITR 2 1 ;
::: ROD3 := GEO: ROD3 SPLITR 2 1 ;
::: ROD4 := GEO: ROD4 SPLITR 2 1 ;
;
*-----
* CASE WITH NO VOID
* Self-Shielding calculation EXCEL
* Transport calculation EXCEL
* Flux TYPE K AND B WITH VARIOUS LEAKAGE OPTIONS
*-----
TRACK INTLIN := EXCELT: CANDU6S ::
TITLE 'TCWD07: CANDU-6 CARTESIAN FUEL TEMP= 941.29'
EDIT 0 MAXR 14 TRAK TISO 7 20.0 SYMM 4 ;
LIBRARY := SHI: LIBRARY TRACK INTLIN ::
EDIT 0 ;
TRACK INTLIN := DELETE: TRACK INTLIN ;
TRACK INTLIN := EXCELT: CANDU6T ::
TITLE 'TCWD07: CANDU-6 CARTESIAN FUEL TEMP= 941.29'
EDIT 0 MAXR 32 ANIS 2 TRAK TISO 7 20.0 SYMM 4 ;
SYS := ASM: LIBRARY TRACK INTLIN ::
EDIT 0 PIJK ;
FLUX := FLU: SYS LIBRARY TRACK ::
TYPE K ;
EDITION := EDI: FLUX LIBRARY TRACK ::
EDIT 3 SAVE COND 4.0 TAKE REGI 1 4 7 10 16 24 ;
FLUX := FLU: FLUX SYS LIBRARY TRACK ::
TYPE B B1 PNL ;
EDITION := EDI: EDITION FLUX LIBRARY TRACK ::
EDIT 3 SAVE COND 4.0 TAKE REGI 1 4 7 10 16 24 ;
FLUX := FLU: FLUX SYS LIBRARY TRACK ::
TYPE B B1 HETE ;
EDITION := EDI: EDITION FLUX LIBRARY TRACK ::
EDIT 3 SAVE COND 4.0 TAKE REGI 1 4 7 10 16 24 ;
FLUX SYS TRACK INTLIN := DELETE: FLUX SYS TRACK INTLIN ;
*-----
* CASE WITH COOLANT VOIDED
* Self-Shielding calculation EXCEL

```

```

* Transport calculation          EXCEL
* Flux TYPE K AND B WITH VARIOUS LEAKAGE OPTIONS
*-----
TRACK INTLIN := EXCELT: CANDU6SV ::
  TITLE 'TCWD07: CANDU-6 CARTESIAN FUEL TEMP= 941.29'
  EDIT 0 MAXR 14 TRAK TISO 7 20.0 SYMM 4 ;
LIBRARY := SHI: LIBRARY TRACK INTLIN ::
  EDIT 0 ;
TRACK INTLIN := DELETE: TRACK INTLIN ;
TRACK INTLIN := EXCELT: CANDU6TV ::
  TITLE 'TCWD07: CANDU-6 CARTESIAN FUEL TEMP= 941.29'
  EDIT 0 MAXR 32 ANIS 2 TRAK TISO 7 20.0 SYMM 4 ;
SYS := ASM: LIBRARY TRACK INTLIN ::
  EDIT 0 PIJK ;
FLUX := FLU: SYS LIBRARY TRACK ::
  TYPE K ;
EDITION := EDI: EDITION FLUX LIBRARY TRACK ::
  EDIT 3 SAVE COND 4.0 TAKE REGI 1 4 7 10 16 24 ;
FLUX := FLU: FLUX SYS LIBRARY TRACK ::
  TYPE B B1 PNL ;
EDITION := EDI: EDITION FLUX LIBRARY TRACK ::
  EDIT 3 SAVE COND 4.0 TAKE REGI 1 4 7 10 16 24 ;
FLUX := FLU: FLUX SYS LIBRARY TRACK ::
  TYPE B B1 HETE ;
EDITION := EDI: EDITION FLUX LIBRARY TRACK ::
  EDIT 3 SAVE COND 4.0 TAKE REGI 1 4 7 10 16 24 ;
FLUX SYS TRACK INTLIN := DELETE: FLUX SYS TRACK INTLIN ;
END: ;
QUIT "LIST" .

```